European Journal of Environmental and Civil Engineering

Volume 27 Number 16 December 2023

Taylor & Francis

ISSN: (Print) (Online) Journal homepage: www.tandfonline.com/journals/tece20

Very high early strength calcium aluminate based binary and ternary cementitious systems: properties, hydration and microstructure

Murat Saydan, Ülkü Sultan Keskin & Burak Uzal

To cite this article: Murat Saydan, Ülkü Sultan Keskin & Burak Uzal (2023) Very high early strength calcium aluminate based binary and ternary cementitious systems: properties, hydration and microstructure, European Journal of Environmental and Civil Engineering, 27:16, 4756-4788, DOI: 10.1080/19648189.2023.2220770

To link to this article: https://doi.org/10.1080/19648189.2023.2220770

EUROPEAN JOURNAL OF ENVIRONMENTAL AND CIVIL ENGINEERING
2023, VOL. 27, NO. 16, 4756–4788
https://doi.org/10.1080/19648189.2023.2220770

Taylor & Francis
Taylor & Francis Group

Very high early strength calcium aluminate based binary and ternary cementitious systems: properties, hydration and microstructure

Murat Saydan[a], Ülkü Sultan Keskin[a] and Burak Uzal[b]

[a]Civil Engineering Department, Konya Technical University, Konya, Turkey; [b]Civil Engineering Department, Abdullah Gul University, Kayseri, Turkey

ABSTRACT

Calcium aluminate cement (CAC) is a cement type that has superior properties such as rapid strength gain, high resistance to high temperatures and harmful chemicals. However, the result of the using of CACs in the production of structural elements occur strength decreases at later ages as a result of a series of chemical reactions called 'conversion reactions' seen in these cements. In this study, the hydration kinetics and the crystalline and amorphous structures formed as a result of hydration were investigated in CAC containing different amounts and types of main oxides-based binary and ternary systems. Considering the results obtained, the main hydration product seen in these specimens was ettringite. Unlike many studies in the literature, metastable structures which cause conversion reactions, such as CAH_{10}, C_2AH_8, have not been observed. Instead of conversion of the phases, ettringite needles were became thin and elongate which causes the paste structure porous and thus causing expansion and strength reduction at the later stages of hydration in some mixtures produce high amounts of ettringite. On the other hand, it is understood that the formation of strätlingite was limited strength decreases in systems where high silica fume is used.

GRAPHICAL ABSTRACT

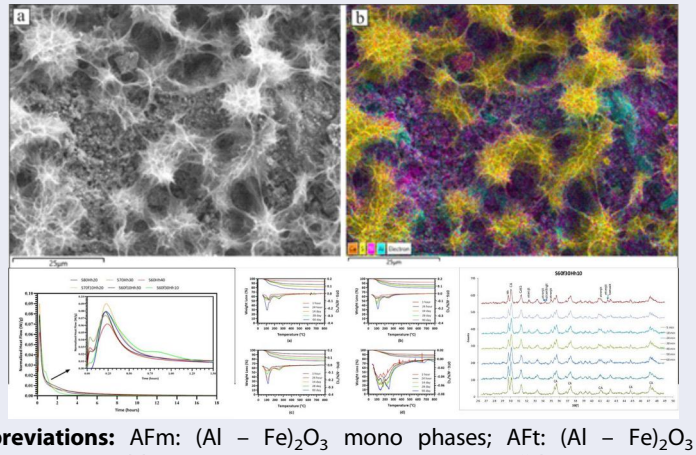

Abbreviations: AFm: $(Al - Fe)_2O_3$ mono phases; AFt: $(Al - Fe)_2O_3$ tri phases; AH_3: Gibbsite; $C_{12}A_7$: Mayenite; C_2ASH_8: Strätlingite; C_3A: Alite; $C_3A.3C\bar{S}H_{32}$: Ettringite; CA: Monocalcium aluminate; CA_2: Calcium

ARTICLE HISTORY
Received 25 August 2022
Accepted 29 May 2023

KEYWORDS
Calcium aluminate cement; ternary systems; rapid strength mortar; dimensional stability; cement microstructure

CONTACT Murat Saydan msaydan@ktun.edu.tr Civil Engineering Department, Konya Technical University, Konya, Turkey.
Supplemental data for this article can be accessed online at https://doi.org/10.1080/19648189.2023.2220770.

dialuminate; CAH: Calcium alumina hydrate; CASH: Calcium alumina silica hydrate; CH: Calcium hydroxide; $C\bar{S}$: $CaSO_4$; Li_2SO_4: Lithum sulphate; Mc: Monocarboaluminate; Ms: Mono sulphoaluminate

1. Introduction

Calcium aluminate cement (CAC) which was first patented in 1888 (Snelus et al., 1888) not only is a different type of cement from ordinary Portland cement (OPC) but also has superior properties than OPC such as rapid strength gain, resistance to high temperatures and temperature changes, resistance to chemical factors, resistance to impact and abrasion (Scrivener & Capmas, 2003; Snelus et al., 1888). Although CAC was developed due to its resistance to sulphate attack in concrete produced with OPC, it was started to be used in many special applications because of its high early strength and refractory properties in the following years (Anderson & Akono, 2017). In the following years, the use of CAC, which was first used in the bearing elements of some structures due to its high strength properties, is prohibited in many countries due to the reactions called 'conversion reactions' that occur especially at later ages and cause strength drops (Mangabhai, 1990; Zhu et al., 2022).

OPC-based systems show a slower but more stable strength development compared to CAC-based systems because of the lower activity of their oxides and the difference of hydration behaviour in the mechanism of induction. On the other hand, CAC-based systems can reach higher strengths than OPC-based systems due to their metastable but very fast hydration reactions in the first hours. Nonetheless, the conversion of metastable phases into stable phases results in an increase in porosity and decrease in strength and this situation was caused the researchers to focus on the elimination of this problem (Deng et al., 2020; Ideker et al., 2019; Lothenbach et al., 2012; Osborne, 1994; Quillin et al., 2001; Singh et al., 1999; Son et al., 2018). The most frequently used method in the literature to limit these strength drops is to support the formation of strätlingite by substituting with supplementary cementitious materials (SCMs), and thus to prevent strength drops. Nevertheless, while the used SCMs gave successful results in preventing strength reductions, it was led to decreases in early strengths.

In the literature, the materials most frequently used together with CACs are OPC, gypsum and various SCMs (granulated blast furnace slag [GBFS], fly ash [FA], silica fume [SF]) (Christensen et al., 2004; Deng et al., 2020; Fernández-Carrasco & Vázquez, 2009; Hidalgo et al., 2009; Osborne & Singh, 1995; Rayment & Majumdar, 1994). The studies examining the reactions of CAC with different SCMs have been started with the collapse of some structural elements produced with pure CAC after losing their strength as a result of conversion reactions and collapsing within 20–25 years (Osborne, 1994). The use of CAC was prohibited in structural elements after some collapses occurred at 1970s in UK. The used materials which form CAC-based binary and ternary systems, can significantly change the hydration kinetics of these systems and the types of hydration products to be formed, depending on the used ratios and the types of materials. Since there are no metastable phases such as C_2AH_8 and CAH_{10} in the systems produced with low ratio of CAC and high ratio of OPC, no decrease in strength is observed at later ages. Thus, the mixtures show similar properties to the mixtures made with OPC. On the other hand, the mixtures in which rich-CAC are used, the same hydrates form as pure CAC mixtures so the properties of the such mixture are very similar to pure CAC systems. The reactions of CAC and OPC in other ratios are more complex, and especially the formation of strätlingite is effective in determining the properties of the mixture (Ideker et al., 2019)

One of the most important problems in mixtures made with CAC and OPC is flash setting. Gu et al. (1994) and Brooks and Sharp (1990) reported that the flash setting in such systems is due to the formation of ettringite in the early stages of hydration. In particular, this flash setting can be seen as a result of mixing CAC with OPC between 20% and 50% (Gu et al., 1997; Zhang et al., 1997). Although the mechanism of the hydration is not fully explained, it is thought that due to the depletion of the sulphate in OPC by reacting with CAC, C_3A in OPC was caused by an uncontrolled reaction with a mechanism similar to a flash setting in PC (Kim et al., 2007; Scrivener, 2003). In order to prevent the flash setting in the binary systems formed from CAC and OPC and the depletion of sulphate in the early stages of hydration, the researchers were created the ternary systems by adding gypsum to the binary systems consisting of CAC and OPC and thus they were able to prevent this flash setting in the early stages of hydration (Torréns-Martín et al., 2013; Torréns-Martín & Fernández-Carrasco, 2013; Zhang et al., 2018). The formation

mechanism of ettringite in CAC-based ternary systems is very important especially in terms of early age strength and setting properties. Ettringite formation occurs when CA and/or C_3A in OPC or CAC react with SO_4^{-} from a sulphate source (gypsum, seawater, groundwater, etc.) as given in Equations (1) and (2).

$$C_3A + 3C\bar{S}H_x + 2CH + (32-3x)H \leftrightarrow C_3A.3C\bar{S}H_{32} \quad (1)$$

$$3CA + 3C\bar{S}H_x + (38-3x)H \leftrightarrow C_3A.3C\bar{S}H_{32} + 2AH_3 \quad (2)$$

As shown in Equation (1), the gypsum placed in the OPC to prevent flash setting reacts with C_3A in the early stages of hydration to form ettringite. This ettringite quickly turns into monosulphate ($C_3A.3C\bar{S}.H_{18}$) after the gypsum is consumed. However, if there is a moisture in the environment, the reactions given in Equations (3) and (4) take places. These reactions are known as AFt-AFm phase conversions.

$$C_3A.CH.H_{18} + 2\ CH + 3\ \bar{S}\ + 11H \leftrightarrow C_3A.3C\bar{S}H_{32} \quad (3)$$

$$C_3A.C\bar{S}.H_{18} + 2\ CH + 2\ \bar{S}\ + 12H \leftrightarrow C_3A.3C\bar{S}H_{32} \quad (4)$$

Another important function of gypsum in binary systems consisting of CAC + Gypsum is to limit the formation of CAH_{10}, which is the metastable phase on the hydration products. It has been observed that almost all types of gypsum can inhibit the formation of CAH_{10}, especially in studies using high amounts of CAC, and therefore, the use of gypsum can limit the strength reductions that occur due to conversion reactions (Li et al., 2020; Son et al., 2019).

The hydration of ternary systems is quite complex because all binders in the system have different chemical and physical properties (Amathieu et al., 2001; Ideker et al., 2019). While gypsum causes ettringite formation in ternary systems as explained above, the stability, formation and the reaction rates of ettringite can easily change depending on the type and amount of gypsum, ambient temperature and humidity (Baquerizo et al., 2016; Brown & Bothe, 1993; Christensen et al., 2004; Hall et al., 1996; Qoku et al., 2017; Renaudin et al., 2010; Xu et al., 2012a, 2012b; Zhou et al., 2004; Zhou & Glasser, 2001). On the other hand, SCMs are another material that is widely used in CAC based ternary systems. The SCMs can also cause complex reactions because it may be contained the large amounts of impurities. In addition to the formation of ettringite in all systems containing CAC and $CaSO_4$, another important hydration product in such ternary systems is strätlingite ($Ca_2Al_2SiO_7.8H_2O$). The strätlingite, which is essentially a silicate AFm phase, is seen naturally in volcanoclastics around the world (Hentschel & Kuzel, 1976; Passaglia & Turconi, 1982) and has taken this name because it was first synthesised artificially by W. Strätling (Okoronkwo & Glasser, 2016a). However, it is more resistant to anions such as OH, Cl, SO_4 and CO_3 because it contains a double layered tetrahedral aluminosilicate interlayer when compared to other AFm phases (Okoronkwo & Glasser, 2016b). This stability, which causes lower AFt-AFm phase transformations compared to other AFm phases, demonstrates the need to support strätlingite formation in such ternary systems (Damidot et al., 2011).

Considering the studies related to SCM containing ternary systems, it may be seen the complexity of the hydration of strätlingite. Midgley and Bhaskara Rao (1978) said that the strätlingite in CAC-based systems may have been formed by the hydration of alumina gel and β-C_2S within the FA or low alumina CAC. This approach has been confirmed by studies showing that in case of the use of pozzolanas that contain highly active Al^{3+} ions such as FA and GBFS it may led to more sulphate attack by increasing the amount of ettringite and strätlingite in the systems (Hou et al., 2018; Hou & Li, 2018). In addition, if sulphate ions are present in the environment at later ages, ettringite formation and sulphate attack can be seen in the mixtures designed by pozzolanic materials containing high alumina content which have not undergone any reaction. This reaction occurs with a reaction similar to the sulphate attack seen in OPC (Mehta & Monteiro, 2014). Furthermore, unlike the hydration of OPC, since there is no CH in the mixture as a result of the hydration of CAC, secondary C-S-H formation is not observed in such ternary mixtures. Instead, SiO_2 from pozzolanas can form the C-A-S-H (strätlingite) structure by entering between the C-A-H structures in CAC (Deng et al., 2020; Majumdar et al., 1990)

Apart from these studies, there are other studies the high PH also support the formation of strätlingite with and increase the thermochemical stability of CAH_{10}, thus limits the strength decreases in later ages (Ding et al., 1995, 1996; Heikal et al., 2004; Kirca et al., 2013).

As mentioned above, there are many studies in the literature on CAC-based binary and ternary systems and their hydration mechanisms. In this researches, a single type of CAC was chosen depend on

the CA content because it is the main oxide of CAC and the hydration mechanism of CA with other binders was examined. It is well known that if Al/Ca ratio is changed in production of CAC, some minor oxides of cement will change and this will cause to exhibit different hydration kinetics of CAC based systems.

The aim of this study is to understand the mechanisms of hydration in binary and ternary systems produced with different CACs that contains different rates of minor and major oxides and their interaction effects of hydration in binary and ternary systems. For this purpose, binary and ternary mixtures were produced with CACs, SF and hemihydrate (Hh) at different mixing ratios. The differences in cement oxides on the strength development and formed hydration products of the ternary systems were also investigated with three different CACs which containing different ratios of effective oxides such that CA, CA_2 and $C_{12}A_7$. In addition, reactions were accelerated using Li_2SO_4 to examine and develop the early strength . in order to observe the hydration products at early ages. The aggregate and gypsum used in the mixtures were determined by preliminary experimental studies. Thus, the differences of hydrate structures caused by the use of different cement oxides of binary and ternary systems have been investigated by various techniques such as *in-situ* and hardened conditions X-ray diffraction (XRD), thermogravimetric analysis (TGA) and field emission scanning electron microscopy (FE-SEM). In addition, the effects of these structures on mechanical behaviour were also examined comparatively. Likewise, it was also investigated the extent to which the hydration kinetics developed or changed at an early age with different mineral and chemical additives by the isothermal calorimetry analysis.

2. Materials and methods

Within the scope of the study, CAC-based binary and ternary systems were prepared. While designing binary systems, gypsum was mixed with CAC at different ratios to ensure the formation of ettringite and to see the effects of different CACs on ettringite. In addition, ternary systems were formed by substituting SF into binary systems to examine the capacity of SCM's to form strätlingite in different CACs. In order to study the hydration mechanisms of the systems during early rapid strengthening and to observe how the transformation reactions develop, the following methodology was considered, respectively;

1. Using CACs with different ratios of oxides in order to examine the effect of different calcium alumina oxides on the hydration kinetics of ternary systems,
2. The use of $CaSO_4$ in the ternary system in order to dominate ettringite in CACs where strength decreases are seen as a result of conversion reactions and thus to reduce metastable phases in hydration products by supporting ettringite formation instead of metastable phases of CACs,
3. To increase the stability of AFt structures and to support the formation of strätlingite, which is known to be stable in the literature, the use of SF, which is known to have a high amorphous silica content, whose effectiveness in ternary systems has not been studied much in the literature,
4. In all systems, adding lithium sulphate (Li_2SO_4) to the systems in order to accelerate early hydration and to examine the effect of the accelerated reaction on the hydration products of the ternary systems from the first minutes (Ye et al., 2022).

2.1. Materials

2.1.1. CAC

In the designed binary and ternary systems, Ciment Fondu, Secar 51 and Secar 71 CACs from Kerneos/Imerys Aluminates company were used which have low, medium and high alumina content, respectively. The oxide components of CACs were determined by XRF and XRD analyzes (Tables 1 and 2).

As mentioned before, the cement main oxides of CACs vary depending on the amount of alumina content. As can be seen in Table 2, CA, $C_{12}A_7$, C_4AF and C_2S ratios are high in Ciment Fondu, CA and C_2AS ratios are high in Secar 51 and CA and CA_2 ratios are high in Secar 71 with low, medium and high levels of alumina, respectively. In this study, the mixtures produced with Fondu, Secar 51 and Secar 71 will be referred to as 'high $C_{12}A_7$ CAC', 'high CA CAC' and 'high CA_2 CAC', respectively, since the effects of different oxide ratios in cements on mechanical and microstructural properties were examined.

Table 1. The oxide composition of CACs as a result of XRF analysis.

	Oxides (% by weight)													
CAC	Al_2O_3	CaO	Fe_2O_3	SiO_2	SO_3	MgO	K_2O	TiO_2	Na_2O	P_2O_5	Cr_2O_3	MnO	OMO	CO_2
Fondu	39.9	37.6	14.3	4.29	0.09	0.32	0.14	1.76	0.06	0.13	0.12	0.10	0.09	1.10
Secar 51	50.5	38.4	1.48	4.62	0.07	0.32	0.25	2.30	0.07	0.11	0.07	0.02	0.12	1.67
Secar 71	68.3	30.2	0.17	0.32	0.02	0.11	0.02	–	0.31	0.01	0.01	–	0.01	0.52

OMO, other minor oxides.

Table 2. Cement compounds and their physical properties as a result of XRD analysis.

	Cement Compounds (% by weight)								
CAC	CA	C_2AS	C_4AF	CA_2	C_2S	C_3A	$C_{12}A_7$	Blaine Fineness (cm^2/g)	Specific weight (g/cm^3)
Fondu	48.3	4.6	13.7	–	7.8	<1	5.6	3407	3.21
Secar 51	66.2	19.2	<1	<1	2.8	<1	1.8	4306	2.99
Secar 71	58.7	<1	–	37.2	<1	–	1.1	3874	2.91

Table 3. The oxide composition and specific weight of SF.

	Oxides (% by weight)										
	SiO_2	MgO	K_2O	Na_2O	Cr_2O_3	SO_3	Fe_2O_3	Al_2O_3	CaO	CO_2	Specific gravity (g/cm^3)
SF	81.1	6.8	3.41	2.71	2.46	0.65	0.55	0.58	0.59	1.15	2.42

2.1.2. Silica fume

The SF was used as a SCM in the designed ternary systems. The used SF was obtained from ETİ Electrometallurgy A.Ş. Antalya/Turkey and its oxide composition and specific weight of SF are given in Table 3.

The biggest feature expected from the SF used is that the SiO_2 in its content has a highly amorphous structure. In order to determine the degree of amorphousness of SF, XRD analysis was performed with Cu anode at 5–65° 2Θ scanning range at a step with 5 deg/min. As a result of XRD analysis, the amorphousness ratio of SF was determined by Mi̇rki̇n (1961) (see Supplementary materials (SM) Equation (S1) and Figure S1 for calculation method and XRD analysis).

The amorphous ratio of SF was calculated as 84%. When looking at the XRD pattern of SF, it is seen that the crystal structures caused by impurities affect the total amorphous ratio of SF. If these crystal structures are not taken into account, the amorphous rate may be higher, but even in this state, the used SF in the mixtures has a high amorphousness rate.

2.1.3. Gypsum

As an SO_4 source, gypsum is the most easily available and the cheapest material in the market. However, there are different types of gypsum. According to the amount of water in their bodies there are three different types of gypsum as anhydrite, Hh and dihydrate. When the literature is examined, it has been seen that these different plaster types have different effects on the hydration of the CAC (Xu et al., 2012a, 2012b; Zhang et al., 2018). On the other hand, dihydrate gypsum has a lower effect on hydration kinetics compared to other gypsum types due to its lower solubility . In this studies, Hh was showed the highest efficiency on CACs (Cecilie & Hansen, 2001; Li et al., 2020; Son et al., 2019; Torréns-Martín & Fernández-Carrasco, 2013).

Within the scope of the study, since a high hydration rate is expected from the prepared systems in the first ages, Hh was used in the mixtures because of their highest dissolution rate (Rolnick, 1954; Tzouvalas et al., 2004). However, there are two different types of Hh as α-Hh and β-Hh. The effects of these gypsum types, which are generally produced with different techniques used during the dehydrating of gypsum (Kelley et al., 1941), on CAC have not been adequately studied in the literature. For this reason, a preliminary trial study was conducted to determine the type of Hh providing the highest performance (see SM Figure S2 for details of preliminary trial).

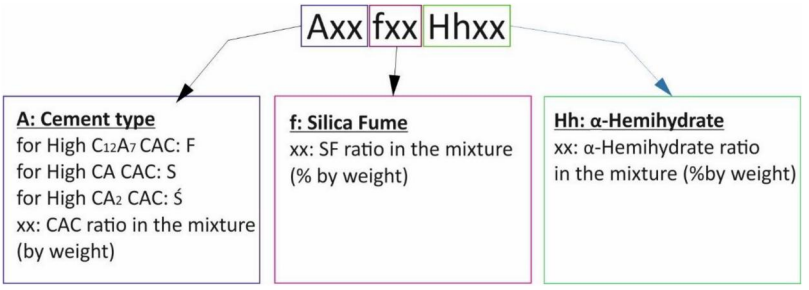

Figure 1. Specimen nomenclature according to ratios of raw materials.

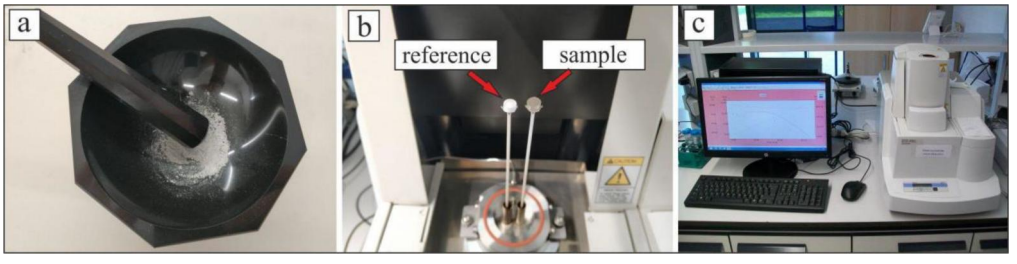

Figure 2. Thermogravimetric Analysis. (a) grinding, (b) holding, (c) device.

As a result of preliminary trial, α-Hh was selected to use in the mixtures to be prepared within the scope of the study, since the compressive strength of the mortars prepared with α-Hh is higher than the β-Hh specimens. α-Hh has been supplied from Nuh Structural Materials Co./Kocaeli-TURKEY.

2.1.4. Crushed marble

The aggregate used in the mixtures was determined by making preliminary trial mixtures, similar to the method followed in the selection of the Hh to be used. Since the strength tests carried out within the scope of the study will be carried out on mortar specimens, aggregates with a maximum diameter of 4 mm with different mineralogical properties and granulometry, which can be easily obtained from the market, were preferred (see SM Table S1, Figure S3 for details of preliminary trial and aggregate specifications). According to the preliminary trial test results, it was decided to use the 'crushed marble' aggregate, which gives the highest compressive strength (see SM Figure S4). The minerological composition of the choosen aggregate was given Table 4.

2.1.5. Water reducing and hydration accelerating agents

Sika® PC 15 (a commercially available product sold by the Sika® Group) was utilised as a water reducing agent. Sika® PC 15 is a modified polycarboxylate-based superplasticiser. The properties of this agent can be found on Sika®'s website.

Another commercially available product, Peramin AXL 80 by imerys group, was used for hydration accelerating purposes. The product contains a minimum of 97% Li_2SO_4. The other product properties can be found on the Imerys group's website.

2.2. Mixture design and recipe

Within the scope of the study, binary and ternary systems were prepared with CAC, α-Hh and SF in varying proportions. Specimen nomenclature was made according to the types and ratios of raw materials used in the mixtures (Figure 1). The mortar specimens were prepared by adding aggregate, water and chemical additives (setting accelerator and water reducer) to the binder, and paste samples were obtained by adding only water and chemical additives. The detailed mixing ratios are given in Table 5.

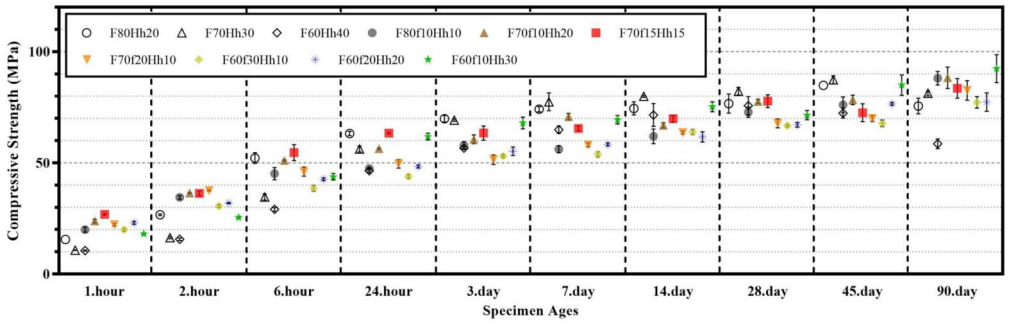

Figure 3. The compressive strength of the specimens produced with $C_{12}A_7$ high CAC.

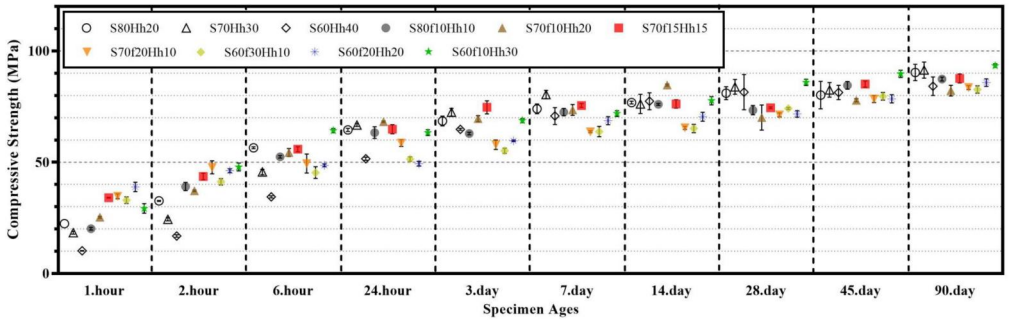

Figure 4. The compressive strength of the specimens produced with CA high CAC.

Table 4. The oxide components and some physical properties of aggregate.

	Oxides (% by weight)									
	CaO	CO_2	SrO	SiO_2	MgO	Al_2O_3	Fe_2O_3	SO_3	Water absorption capacity (%)	Specific weight (g/cm^3)
Crushed Marble 2	61.0	38.7	0.02	0.25	0.07	0.17	0.05	0.01	0.49	2.67

2.3. Methodology

2.3.1. Preparation of the specimens

The mortar cube specimens of size $50 \times 50 \times 50$ mm for compressive strength test and the mortar bar specimens of size $25 \times 25 \times 285$ mm for dimensional stability test were casted and cured under 99% relative humidity and 20 ± 1 °C temperature environment. Also paste samples of size 20*40*20 mm for the microstructure analysis were casted and stored same conditions. The mortar specimen mixtures were made with a laboratory mixer and the paste sample mixtures were made with a hand mixer. In both specimen types, water, water reducer additive and Li_2SO_4 were mixed together with a fast mixer at 800 rpm and added to the blended binder in the form of suspension.

2.3.2. Mechanical tests

In the present study, the compressive strength and dimensional stability tests were made on the prepared mortar specimens. In addition to the results obtained from the tests, repeated non parametric multivariate variance analysis (PERMANOVA) were performed depend on normality tests on data (Anderson, 2017; Hand & Taylor, 1987). The multiple significance tests and analysis of variance were determined by assigning the material ratios used in the mixtures as independent group variables. The multivariate variance analysis was studied in SPSS and PAST software at 95% confidence level.

Table 5. Mixing ratios of the specimens.

	Binary and ternary systems					Additives		Mixture ratios	
	Cement type % by wt			SCM % by wt	Gypsum % by wt	For mortar (for paste) % by weight cement amount			
Specimens Nomenclature	$C_{12}A_7$ high CAC	CA High CAC	CA_2 High CAC	SF	α-Hh	Li_2SO_4	Superplasticizer	Water/ binder	Binder/ aggregate
F80Hh20	80	0	0	0	20	1	2(1)	0.3	0.5
S80Hh20	0	80	0	0	20	1	2(1)	0.3	0.5
Ś80Hh20	0	0	80	0	20	1	2(1)	0.3	0.5
F70Hh30	70	0	0	0	30	1	2(1)	0.3	0.5
S70Hh30	0	70	0	0	30	1	2(1)	0.3	0.5
Ś70Hh30	0	0	70	0	30	1	2(1)	0.3	0.5
F60Hh40	60	0	0	0	40	1	2(1)	0.3	0.5
S60Hh40	0	60	0	0	40	1	2(1)	0.3	0.5
Ś60Hh40	0	0	60	0	40	1	2(1)	0.3	0.5
F80f10Hh10	80	0	0	10	10	1	2	0.3	0.5
F70f10Hh20	70	0	0	10	20	1	2(1)	0.3	0.5
F70f15Hh15	70	0	0	15	15	1	2	0.3	0.5
F70f20Hh10	70	0	0	20	10	1	2	0.3	0.5
F60f10Hh30	60	0	0	10	30	1	2(1)	0.3	0.5
F60f20Hh20	60	0	0	20	20	1	2	0.3	0.5
F60f30Hh10	60	0	0	30	10	1	2(1)	0.3	0.5
S80f10Hh10	80	0	0	10	10	1	2	0.3	0.5
S70f10Hh20	70	0	0	10	20	1	2(1)	0.3	0.5
S70f15Hh15	70	0	0	15	15	1	2	0.3	0.5
S70f20Hh10	70	0	0	20	10	1	2	0.3	0.5
S60f10Hh30	60	0	0	10	30	1	2(1)	0.3	0.5
S60f20Hh20	60	0	0	20	20	1	2	0.3	0.5
S60f30Hh10	60	0	0	30	10	1	2(1)	0.3	0.5
Ś80f10Hh10	80	0	0	10	10	1	2	0.3	0.5
Ś70f10Hh20	70	0	0	10	20	1	2(1)	0.3	0.5
Ś70f15Hh15	70	0	0	15	15	1	2	0.3	0.5
Ś70f20Hh10	70	0	0	20	10	1	2	0.3	0.5
Ś60f10Hh30	60	0	0	10	30	1	2(1)	0.3	0.5
Ś60f20Hh20	60	0	0	20	20	1	2	0.3	0.5
Ś60f30Hh10	60	0	0	30	10	1	2(1)	0.3	0.5

2.3.2.1. Compressive strength test. The compressive strength tests of the specimens were carried out according to ASTM C109/C109M-21 (2020). The cured cubic specimens were subjected to compressive strength test at 1, 2, 6 and 24 h and 3, 7, 14, 28 and 90 days (considering the time when water is added to the mixtures). The compressive strength test was performed on three specimens for each age and group and mean compressive strengths were obtained.

2.3.2.2. Dimensional stability test. Length changes of $25 \times 25 \times 285$ mm prismatic mortar bars are determined according to ASTM C490/C490M-21 (2021) standard. The length changes of prismatic mortar bars, which were kept in the same conditions with cube specimens, were measured with a digital comparator at 1, 2, 6, 24 h and 3, 7, 14, 28, 45, 90th days starting from the addition of water to the mixtures. Two prismatic specimens were prepared for each group and the results were recorded as the average of the two samples. The length values of the specimens read at the end of the first hour were accepted as L_0 and the relative length changes (in percent) of the samples were determined accordingly (Equation 5).

$$\text{Relative Length Change} = \frac{L_x - L_0}{L_0} \times 100 \tag{5}$$

where;
L_x = Length of the 'x' age specimen
L_0 = Length of the specimen at the end of the first hour

2.3.3. Microstructural analysis and determination of hydration kinetics

Hydration kinetics and microstructural properties of the systems were determined on fresh and hardened paste specimens.

2.3.3.1. Isothermal calorimetry analysis. Because the hydration of cements is an exothermic reaction, it is quite suitable to be measured by isothermal calorimetry. Determining the exothermic energy resulting from hydration with isothermal calorimetry is a useful qualitative method in terms of evaluating hydration kinetics and factors affecting hydration.

Within the scope of the study, isothermal calorimetry analyzes were carried out at 20 ± 1 °C with TAM Air isothermal calorimetry. A total of 7 g of each sample was mixed outside the calorimeter (*ex-situ*) throughout 15 s in polypropylene ampoules and then was placed in the calorimeter. The analysis was continued for 22 h.

2.3.3.2. Thermogravimetric analysis. TGA analyzes of the samples were performed with the DTG-60H simultaneous DTA-TG device of Shimadzu Co. (Kyoto, Japan) (Figure 2c). The hydration of the samples was stopped with isopropyl alcohol for to determine not the free water in the sample but the amount of bound water in the hydrated compounds. Then, approximately 50 mg of samples were placed in a platinum sample cup (Figure 2b) after the samples were ground to a powder with an agate mortar (Figure 2a). The sample was heated from room temperature to 800 °C at a rate of 10 °C/min in 99.5% pure N_2 gas flow (10 mL/min).

2.3.3.3. XRD analysis. Within the scope of the study, XRD analysis was performed on the paste samples produced with two different techniques. *In-situ* XRD analysis was performed on the samples during the first hour in order to see the formation of the phases within 1 h after the start of hydration, since very fast early strength is expected from the produced samples. A special silicone sample holder was used to perform XRD analysis *in situ*. The sample were placed in the XRD device immediately after two minutes of mixing with water and the first analysis was carried out immediately. Then, the analyze was repeated every 10 min until the 60th minute based on the time of adding water to the sample. A high resolution Lynxeye detector was used to better see the differences between patterns in analysis.

Besides in-situ analysis of fresh paste, XRD analysis of aged samples was performed on specimens whose hydration was stopped in order to be compatible with FE-SEM imaging and TGA. The analyzes were carried out on the samples obtained by pelleting the powdered specimens with an agate mortar.

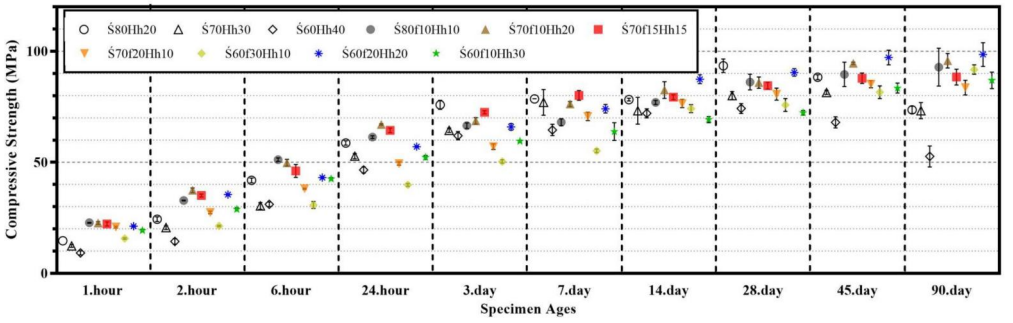

Figure 5. The compressive strength of the specimens produced with CA_2 high CAC.

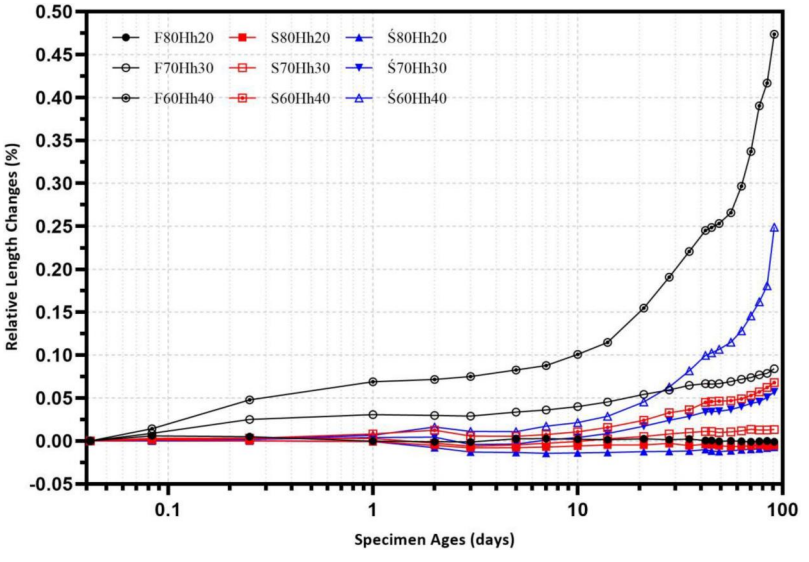

Figure 6. The relative length changes of binary systems.

XRD analyzes on both *in situ* and hardened samples were performed on Bruker D8 Discover with CuKα anode at $\lambda = 1.54$ Å wavelength. The scanning range parameter was setted at 5° to 90° (2Θ), 0.020° scan step length and 0.014 s/step scanning speed. It has been studied at power and energies of 40 kV and 40 mA in X-Ray source.

Although, quantitative phase analyzes of crystal structures on XRD patterns were performed according to the reference intensity ratios method, which is a modified version of the internal standard method, with the diffrac.eva software (Chung, 1973). Using the ICDD pdf 4+ reference databases and the diffrac.eva software, the quantitative analyzes of the phases were determined according to equation developed by Hubbard and Snyder (1988).

2.3.3.4. FE-SEM imaging and EDX analysis. Within the scope of the study, FE-SEM imaging was performed on the samples, which were cut and polished very thinly and the hydration was stopped and dried, with the GeminiSEM 500 device of Zeiss, and EDX analysis was performed with the UltimExtreme EDX device of the Oxford instruments co. In order to better visualise the surface topography, FE-SEM was carried out in-lens mode and at 1 kV energy. Thus, the surface images of hydrated structures could be obtained with higher resolution. The surfaces of the samples are coated with 4–5 nm—thick iridium before imaging.

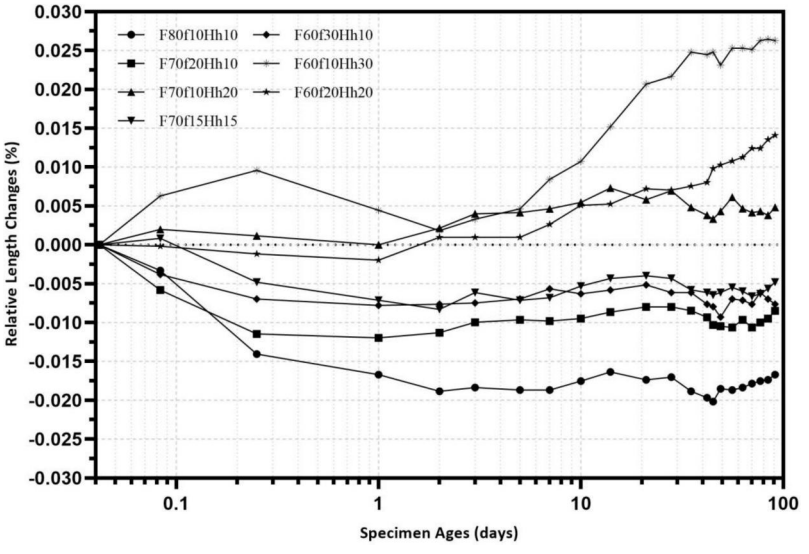

Figure 7. The relative length changes of the ternary systems produced with $C_{12}A_7$ high CAC.

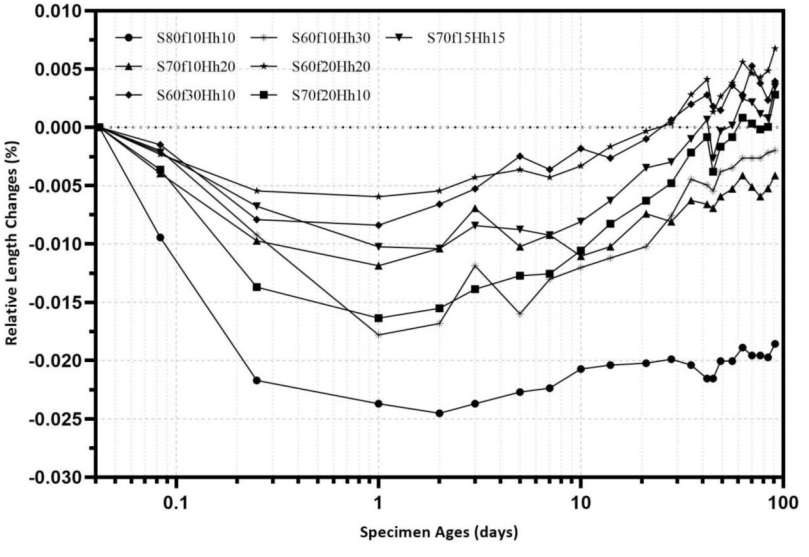

Figure 8. The relative length changes of the ternary systems produced with CA high CAC.

3. Results and discussion

3.1. Mechanical test results

The compressive strength test results of the binary and ternary systems were given in Figures 3–5.

From the results, it was observed that the increase in the amount of CA in the cement was increased the early age compressive strength, whereas the increase in the amount of CA_2 was decreased this strength. On the other hand, the late-age compressive strengths of ternary systems produced with 70% by weight CA_2 high CAC were higher than the specimens produced with other CACs. Moreover, the addition of SF was clearly increased the compressive strength of mortars, especially at early age, compared to the binary systems. Although while SF have been regulated the compressive strength development of the mortars, it has decreased the late-age compressive strengths of the mixtures except prepared with CA_2 high CAC.

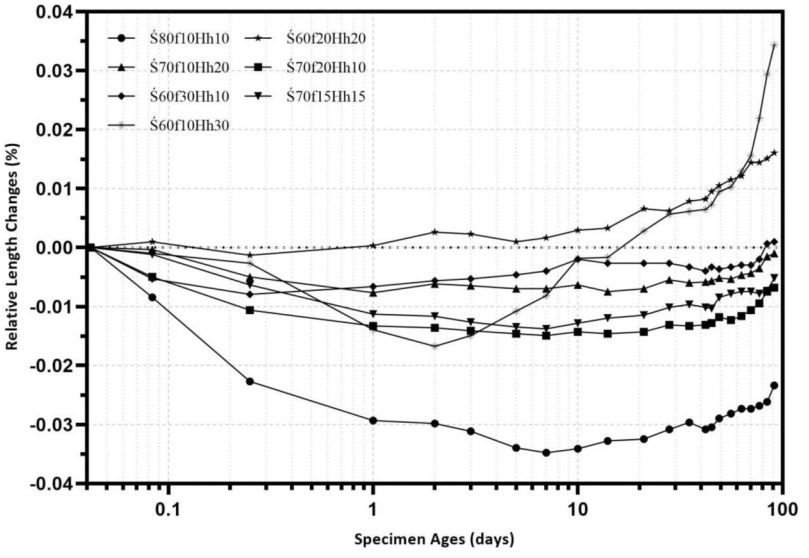

Figure 9. The relative length changes of the ternary systems produced with CA_2 high CAC.

Table 6. Normality tests and two way PERMANOVA analysis.

Dependent variables		Repeated measure	Independent variables	Multivariate normality test (omnibus)	Box-M test	Effects		Mahalanobis *F* Value	Mahalanobis *p* Value
Depend on Compressive Strength	Results of $C_{12}A_7$ high CAC CA high CAC CA_2 high CAC	Cement type	Hh	0.10	0.0005	Main	Hh	0.948	0.0015*
			SF				SF	0.597	0.0483*
						Interact	Hh*SF	−2.813	0.7334
Depend on Dimensional Stability	Results of $C_{12}A_7$ high CAC CA high CAC CA_2 high CAC	Cement type	Hh	10^{-34}	0.0005	Main	Hh	3.086	0.001*
			SF				SF	3.084	0.004*
						Interact	Hh*SF	−3.021	0.999

*Significant.

When the compressive strength results are examined, the obtained values reveal that the oxide phases of cement have a direct effect on the compressive strengths. Among these phases, the setting time of the mortars produced with $C_{12}A_7$ high CAC is quite short due to the rapid reaction of the $C_{12}A_7$, which is very reactive compared to the other aluminate phases (Singh & Glasser, 1988), but the $C_{11}A_7.Ca(OH)_2$ formed as a result of the hydration of this phase does not have a positive effect on strength (Singh & Glasser, 1988). Contrary to $C_{12}A_7$, CA_2 is a phase that has a slow hydration and can take a long time, as mentioned before. This situation also explains the decrease in early age compressive strength of the ternary systems produced with CA_2 high CAC. The early-age strength of mortars produced with CA high CAC were showed to be quite high among the cements used.

SF has considerably increased the early age compressive strength of the ternary systems, even if it is used in small amounts. Especially, while the amount of SF used in the mixtures increases, the decrease in the late-ages strength of the specimens suggests that SF causes a filling effect in the mixtures rather than reacting with CAC. However, the high late-age compressive strength of ternary systems produced with CA_2 high CAC and a high amount of SF was distorted this estimation.

The dimensional changes of binary systems relative to each other is given in Figure 6, and comparison of dimensional changes of ternary systems is given in Figures 7–9.

The increase in the amount of Hh in binary systems caused expansion in the specimens. The expansions were much higher in the specimens produced with especially high ratios of Hh (>30%) and $C_{12}A_7$ or CA_2 high CAC compared to other specimens. The highest expansion was observed as 0.473% on the 91st day in the sample containing 60% $C_{12}A_7$ high CAC and 40% Hh by weight. However, even this

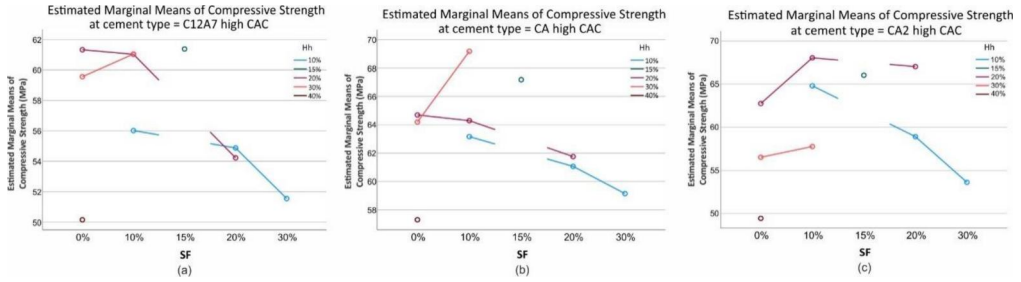

Figure 10. Relationship of SF and Hh with estimated marginal means of compressive strengths as a result of PERMANOVA statistics. (a) produced with '$C_{12}A_7$ high CAC', (b) produced with 'CA high CAC', (c) produced with 'CA_2 high CAC'.

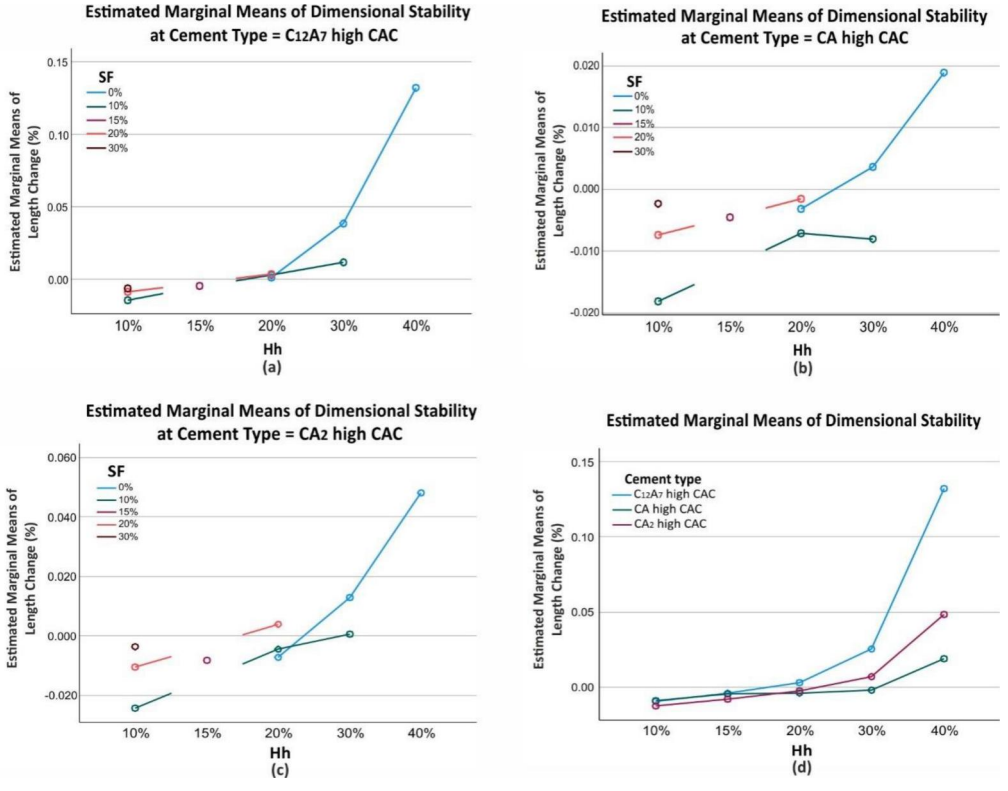

Figure 11. Relationship of SF and Hh with estimated marginal means of relative length changes as a result of PERMANOVA statistics. (a) produced with '$C_{12}A_7$ high CAC', (b) produced with 'CA high CAC', (c) produced with 'CA_2 high CAC' (d) Effect of Hh on different CAC types.

highest expansion did not exceed the crack threshold value in the samples and thus did not cause any crack. The crack threshold value can be accepted as the point where the intrinsic tensile stresses caused by expansions exceeded the maximum tensile strength (Lu et al., 2023). Especially, the expansion rates in all binary systems have increased even more after the 45 days. On the other hand, the shrinkage occurred between the 1 h to the 45 days in binary mortar systems contained low amount of Hh, except those produced with $C_{12}A_7$ high CAC.

In the ternary systems examined, it is seen that different length changes occur in different CAC types and Hh amounts. When looking at Figure 7, the expansions has been seen at the first hours in the specimens produced with $C_{12}A_7$ high CAC and contained more than 10% Hh by weight. The shrinkage was occurred to be inversely proportional to the amount of SF from 6 h up to 3 days in the specimens. After

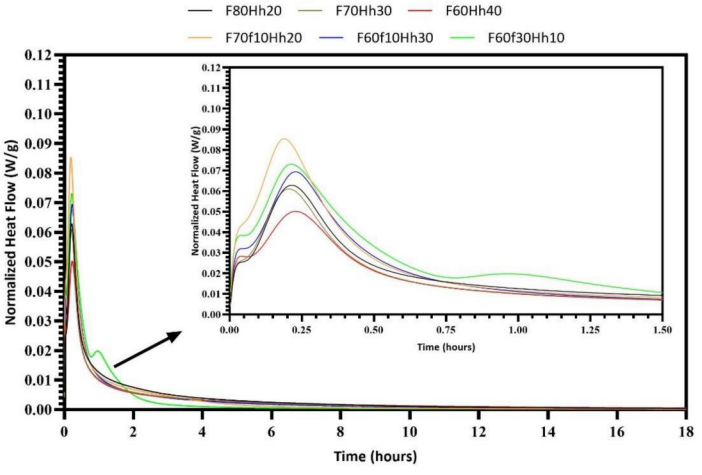

Figure 12. The heat flow curves of specimens produced with '$C_{12}A_7$ high CAC'.

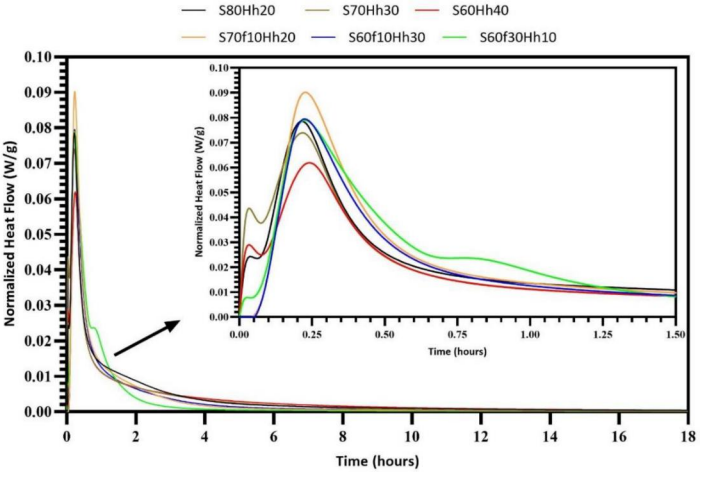

Figure 13. The heat flow curves of specimens produced with 'CA high CAC'.

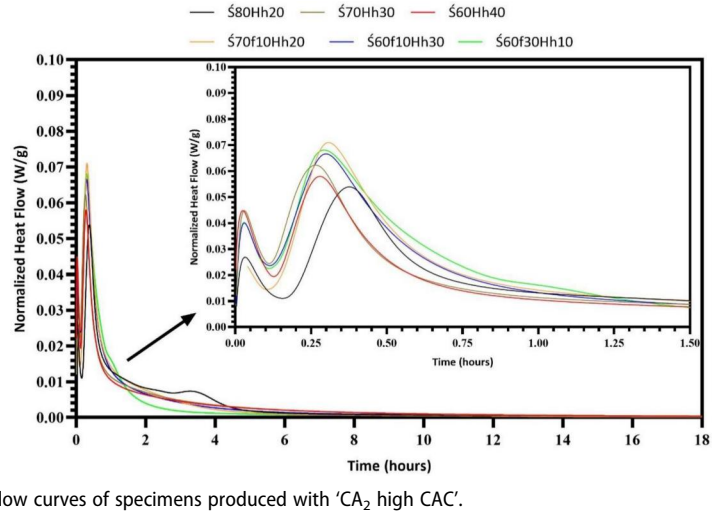

Figure 14. The heat flow curves of specimens produced with 'CA_2 high CAC'.

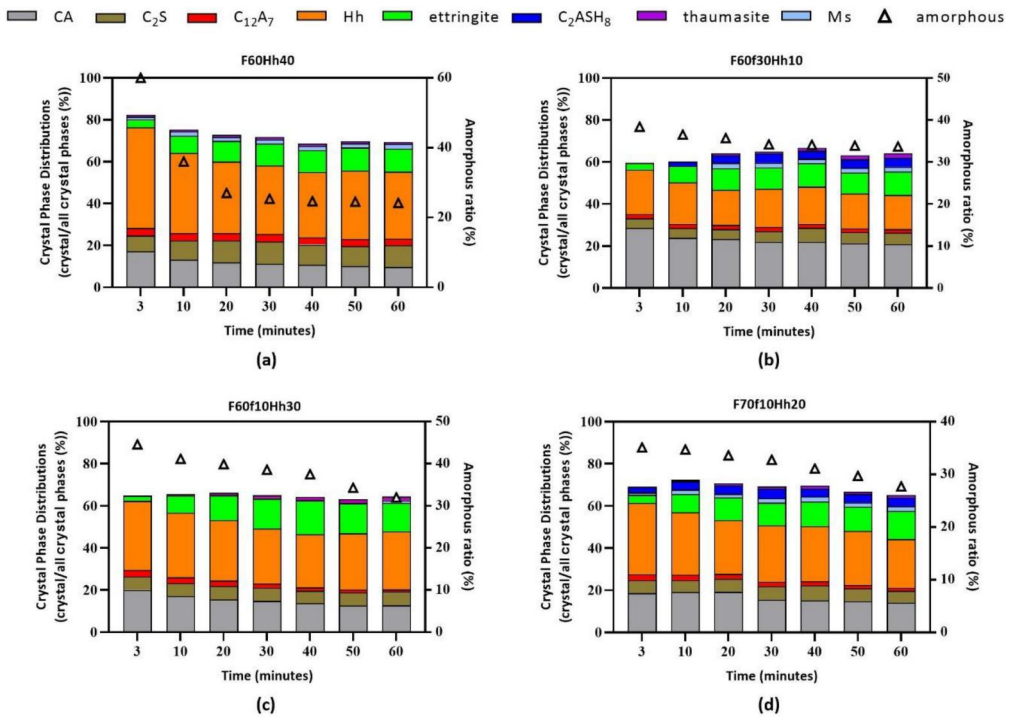

Figure 15. The crystal phase distributions and the amorphous ratios of samples produced with '$C_{12}A_7$ high CAC' (in-situ XRD analysis).

the 3 days, the expansion was started to increase in the specimens containing high Hh, however, no significant shrinkage or expansion was observed in the other samples.

In ternary systems prepared with CA high CAC, the shrinkage was occurred from the first hour to the 24 h, unlike the specimens prepared with $C_{12}A_7$ high CAC as can be seen Figure 8. After the 24 h, the length of the specimens was continued to expanding with increasing slopes. Similarly, with ternary systems formed CA high CAC, the systems produced with CA_2 high CAC were also shown generally shrinkage in the first 3 days, and the expansion was dominated the systems until the 91 days (Figure 9).

In addition, when all binary and ternary systems were examined, it was observed that the increase in cement ratios was reduced the expansion of the specimens and even it was caused shrinkage in most cases at late-ages. On the contrary, the expansions dominated the dimensional properties in systems using less cement by ratio. Considering to this situation, it is evaluated that the increase in the CAC/Hh ratio in the mixtures was caused shrinkage. On the other hand, although the decrease of this ratio was generated the expansion in late-ages, the shrinkage occurs in the early stages of hydration. In addition, it is understood from the graphs given in Figures 7–9 that SF does not have a direct effect on the length changes of the specimens in terms of expansion and shrinkage. However, it can be seen that the length changes in the specimens using 60% CAC, 30% SF and 10% Hh in all CAC types were proportionally lesser than containing 60% CAC, 30% Hh and 10% SF. In particular, this supports the idea that the addition of SF not only shows a filler effect but also reduces the amount of metastable or expansion-sensitive AFm-AFt phases in the systems, thus limiting expansion and shrinkage.

On the other hand, the effects of Hh and SF ratios on compressive strength and dimensional stability in terms of main and interaction effects were investigated using PERMANOVA analysis. The results obtained from the analysis of variance are given in Table 6. The PERMANOVA statistics, which is a much more flexible method than parametric variance analysis, was used since the data do not comply with multivariate normality and/or sphericity and homogeneity test (Tang et al., 2016). The p value $<$ .05 was accepted that the independent variable with had a significant effect on the dependent variable. Since the p value less than .05, the independent variable has significant on the dependent variables was accepted. Contrary to this situation, since the p values obtained in the normality and Box-M

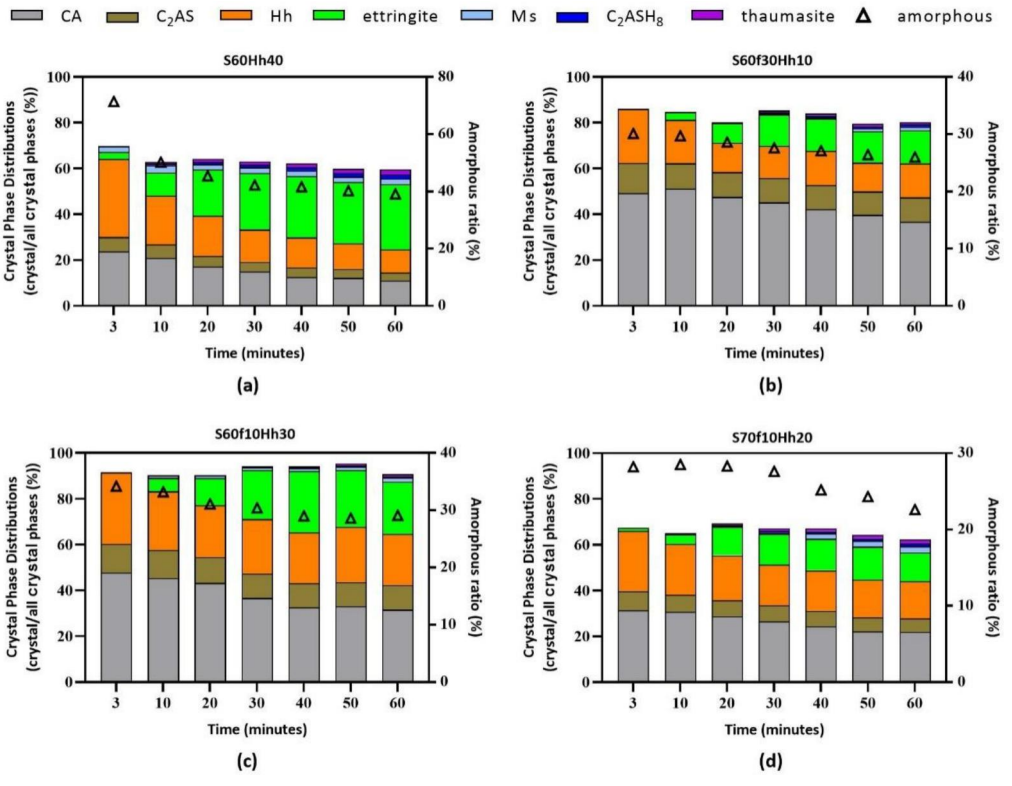

Figure 16. The crystal phase distributions and the amorphous ratios of samples produced with 'CA high CAC' (in-situ XRD analysis).

tests were less than .05, the H_0 hypothesis was rejected and the data was not comply with this assumptions.

The main effects of Hh and SF on the dependent variables were shown in Figures 10 and 11. Interaction effect of SF and Hh were not significant on the results but the main effect of both was significant. The compressive strength and dimensional stability results were highly affected from Hh and SF ratios. In addition, Hh has a higher effect on both results. Although SF had an increasing effect on the compressive strength of the samples at early ages, it was decreased the compressive strength at middle and later ages (see SM Figure S5). The effect of Hh on early strengths may have increased due to the accelerating effect of Li_2SO_4 (Sun et al., 2022). The increase in the Hh ratio was caused the expansions on the specimens. In contrast to Hh, the increase in SF ratios were limited the length changes in the specimens. On the other hand, the type of CAC shows significant differences on the results depending on the raw material ratios. Especially in CA high CAC, the increase in SF ratio from 0% to 10% was resulted in higher strength increases compared to the other two cement types. Apart from this, the decrease in CAC ratios or the increase in SF ratios were caused decreases in compressive strengths. It is an expected situation that the amount of hydrated products will decrease due to the decrease in the amount of cement. Therewithal, the specimens produced with $C_{12}A_7$ high CAC has expanded much more than others.

3.2. Analysis of microstructure

3.2.1. Hydration kinetics

The heat flow curves in the systems were obtained as a result of calorimetry analysis on the samples selected for microstructural analysis given in Figures 12–14.

It is seen in Figure 12 that the first peak formed due to the rapid dissolution of Hh in the systems prepared with $C_{12}A_7$ high CAC is almost intertwined with the second peak formed as a result of the

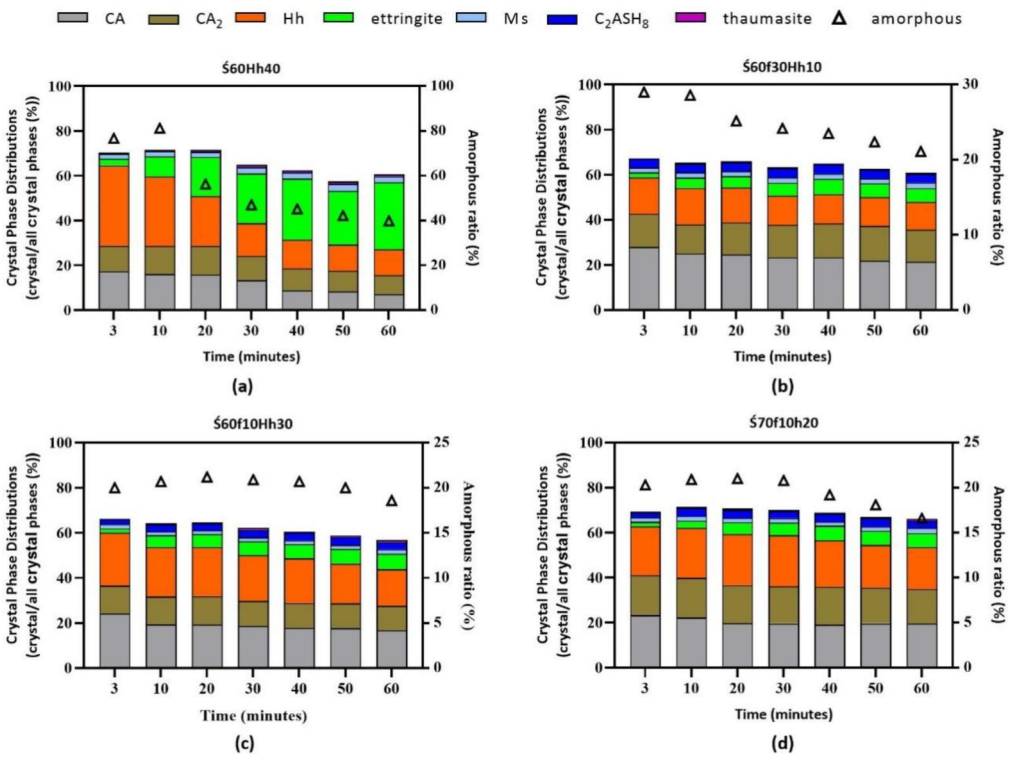

Figure 17. The crystal phase distributions and the amorphous ratios of samples produced with 'CA_2 high CAC' (in-situ XRD analysis).

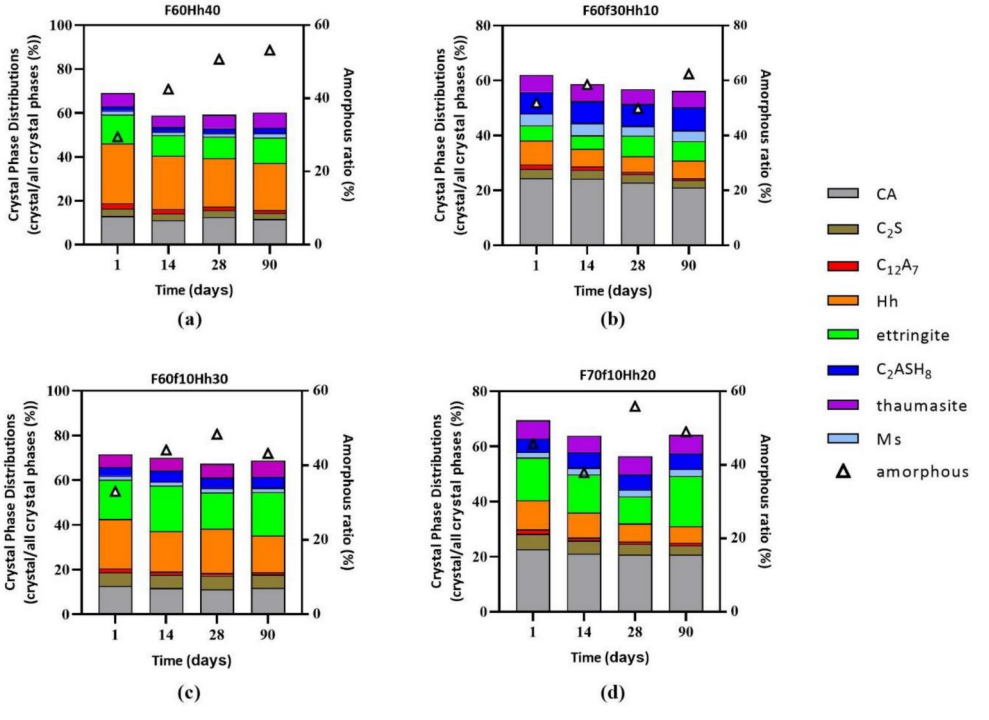

Figure 18. The crystal phase distributions and the amorphous ratios of samples produced with '$C_{12}A_7$ high CAC'.

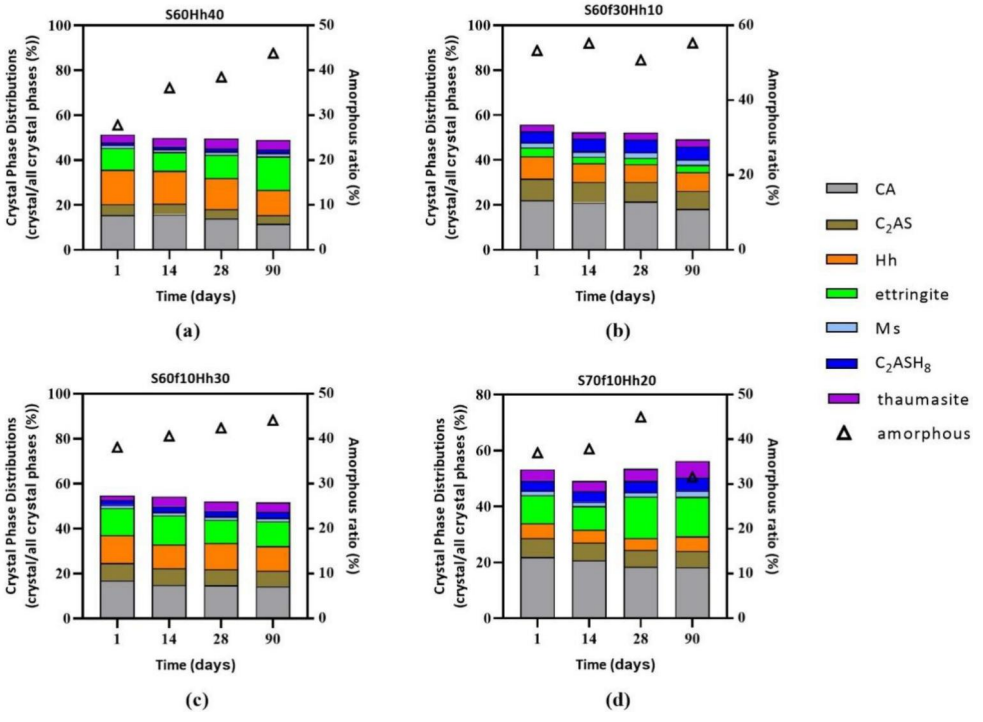

Figure 19. The crystal phase distributions and the amorphous ratios of samples produced with 'CA high CAC'.

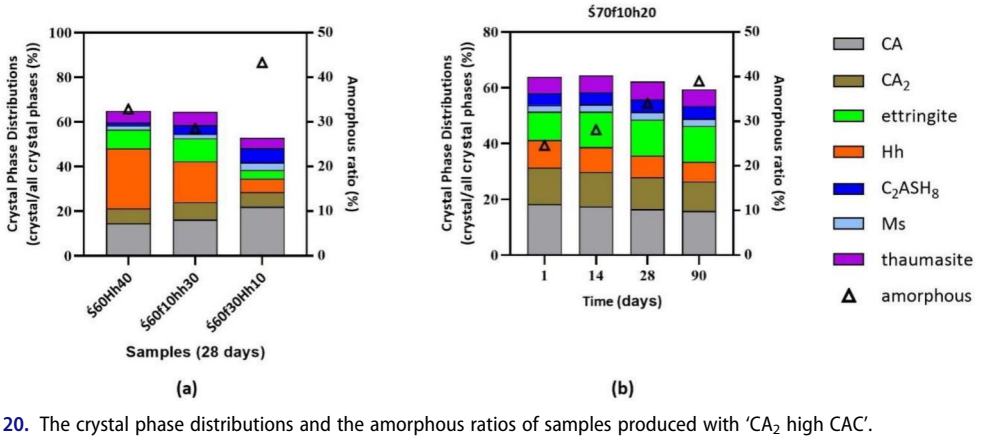

Figure 20. The crystal phase distributions and the amorphous ratios of samples produced with 'CA_2 high CAC'.

dissolution of the $C_{12}A_7$, and the precipitation of the first hydration products. This situation was more evident in systems produced with CA high CAC due to a slight shift of the second peak to the right (Figure 13). Similar to this case, the first peaks became highly visible because the second peak shifted more to the right in systems produced CA_2 high CAC (Figure 14). When looking at all the graphs, it can be easily said that this interpenetration is due to the differences on the dissolution and precipitation rates of the cement oxides rather than the dissolution of Hh. If this situation is explained with the oxides of the used CACs, the dissolution period was occurred at the highest rate in the samples produced with $C_{12}A_7$ high CAC, which causes a fast reaction, and on the contrary, the slowest rate of dissolution was observed in CACs containing high amount of slow-reacting CA_2. As stated by Rodger and Double (1984) and Capmas et al. (1990), the induction period required in order for the hydrated phases to precipitate, where starts with the dissolution of the calcium aluminate phases in water and ends with the Ca_2^+ and $Al(OH)_4^-$ ions

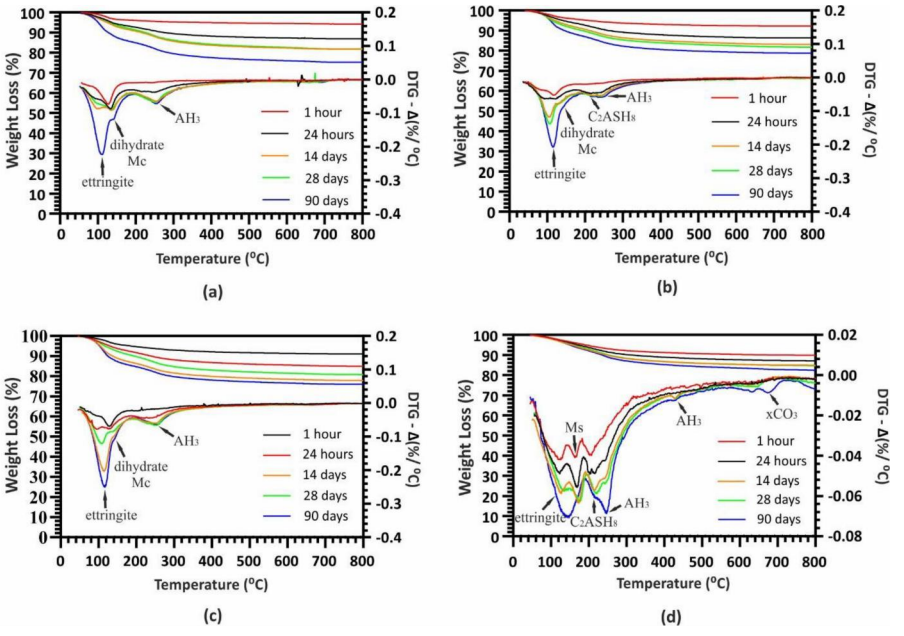

Figure 21. The DTG curves and total weight loss due to dehydration of the samples (a) F60Hh40, (b) F60f10Hh20, (c) F60f10Hh30, (d) F60f30Hh10.

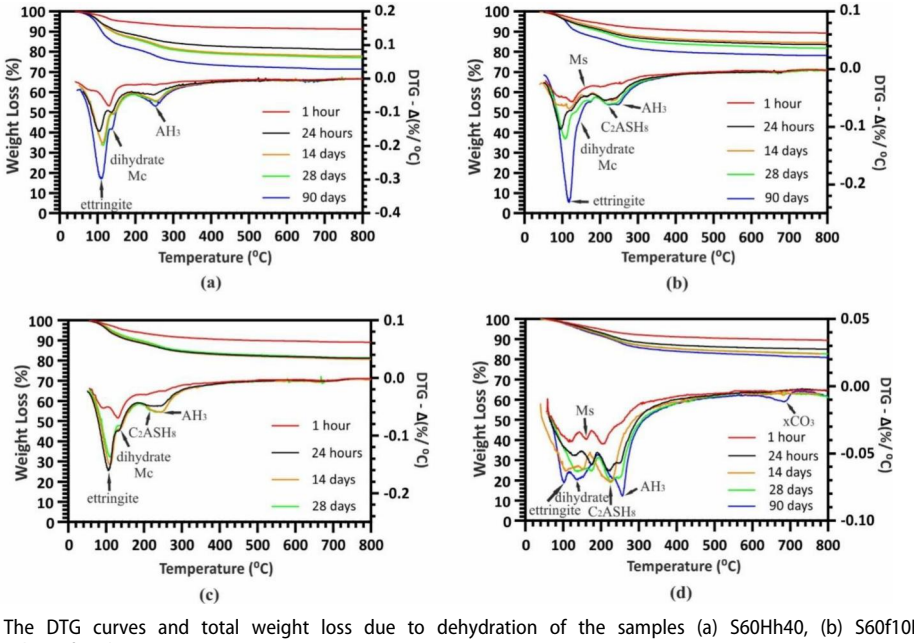

Figure 22. The DTG curves and total weight loss due to dehydration of the samples (a) S60Hh40, (b) S60f10Hh20, (c) S60f10Hh30, (d) S60f30Hh10.

reaching a certain concentration in the solution, occurred together with the other periods and without any delay because the effect of Li_2SO_4.

On the other hand, when the mixtures with the same cement ratios by weight are taken into consideration, the SF increased the maximum heats of ternary systems containing SF relative to binary systems, between 28% and 32%, 23% and %25, 11% and 13% in systems produced with $C_{12}A_7$ high CAC, CA high CAC and CA_2 high CAC, respectively. It is possible to explain this effect of SF, which affects hydration

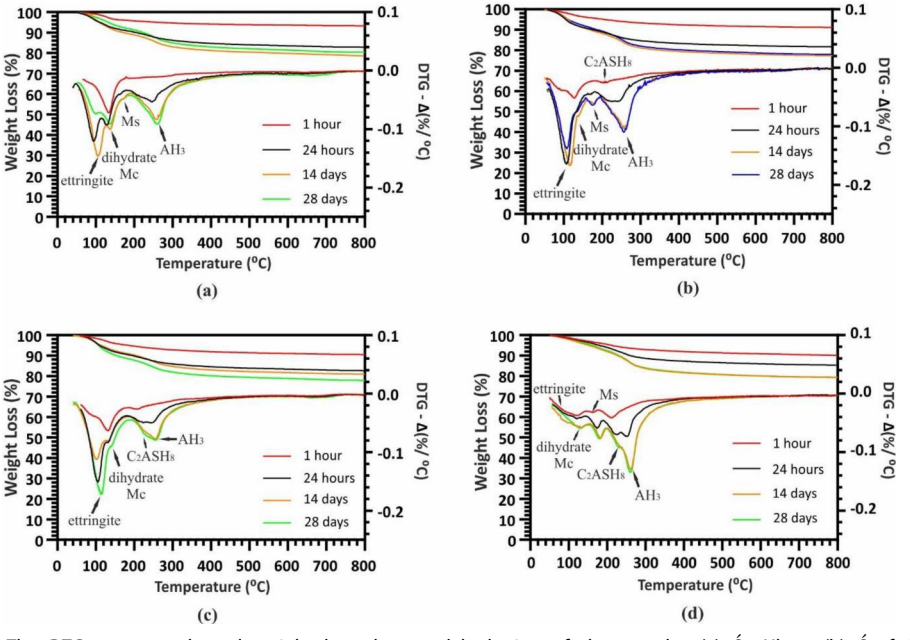

Figure 23. The DTG curves and total weight loss due to dehydration of the samples (a) Ś60Hh40, (b) Ś60f10Hh20, (c) Ś60f10Hh30, (d) Ś60f30Hh10.

rates, in two ways (Bizzozero, 2014): (1) Because of it has particles smaller than cement, SF provided extra nucleation area for hydrates to form in the solution. This was significantly accelerated the hydration especially in the first minutes and thus the amount of hydrated product increased in the same time. (2) SF also showed a diluting effect in mixtures, allowing enough space for the hydrates to grow and reach the appropriate concentration in the solution.

When looking at all mixtures, the third peak indicating sulphate depletion occurred in ternary systems containing 60% CAC, 30% SF, 10% Hh and binary systems containing 80% CA and/or CA_2 high CAC and 20% Hh. Sulphate depletion is an expected situation, since the system containing 60% CAC, 30% SF, 10% Hh has the highest CAC/Hh ratio among the systems. Gosselin (2009) has shown that increasing the water/cement ratio reduces the slope of the deceleration period of the second peak, in other words, it was decreased the reaction rate. Based on this study, it could be said that the absence of the third peak in other mixtures with high CAC/Hh ratios may be due to the rapid and early completion of the hydration, because the water/binder ratio ($w/b = 0.3$) was low in these mixtures. On the other hand, unlike the binary systems prepared with CA or CA_2 high CAC, the third peak does not appear in the binary systems prepared with 80% $C_{12}A_7$ high CAC and 20% Hh. This was shown that the amount of CA was also quite effective in terms of sulphate depletion

3.2.2. Hydration products and phase compositions

XRD analyses were carried out on both *in situ* and hardened samples, and TGA analyses were only carried out on hardened samples so that free water would not affect the analysis parameters, and the phase compositions and hydration products were examined. Accordingly, from the XRD analyzes performed between 0 and 60 min of *in-situ* samples, it is seen that the main phase that starts to form from the first minutes of hydration in all prepared binary and triple system samples is ettringite (Figures 15–17). In binary and triple systems prepared with $C_{12}A_7$ or CA high CACs, ettringite formation started from the 10th minute and continued to increase continuously throughout the 60-minute analysis period (Figures 15 and 16). In the mixtures prepared with CA_2 high CAC, the peaks showing the formation of ettringite started to occur 20 min after the start of hydration (Figure 17). Apart from the formation of ettringite, other important phases seen in the mixtures are AFm phases such as monosulphoaluminate (Ms), hydrocalumite and thaumasite. It can be said that these structures were formed more in samples where Hh is

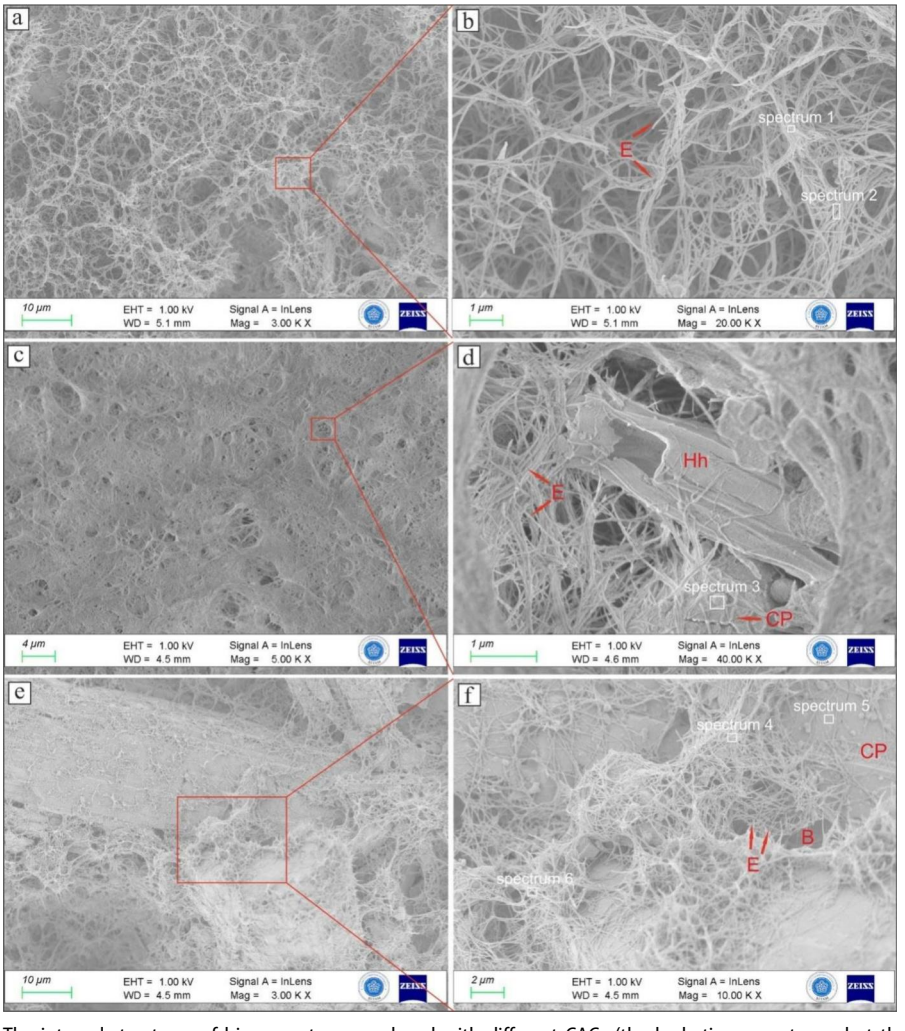

Figure 24. The internal structures of binary systems produced with different CACs (the hydration was stopped at the 1st hour). (a, b) F60Hh40, (c, d) S60Hh40, (e, f) Ś60Hh40. (E, ettringite; Hh, hemihydrate; CP, cement particles; B, void) (the scales of the images are different).

used less. However, due to the low water/binder ratio (0.3) chosen in the mixtures, it is also striking that Hh and CA were not completely consumed in many systems since the hydration reaction slowed down very early. In short, the most important parameter limiting the hydration in the systems was the water/-binder ratio. Strätlingite, which is expected to form in the systems and is a more stable structure than ettringite, was formed in all samples, especially in samples containing high amounts of SF. However, apart from the dominant ettringite precipitation, the formation of other phases remained very limited.

Besides these phases, phases such as CAH_{10}, C_2AH_8, AH_3 and C_3AH_6, which are expected to occur as a result of hydration of CACs, were not observed in the prepared binary and ternary systems either in the first hours or in the late age of hydration. On the other hand, these phases are not easily detectable experimentally because they have weak crystal structures or are easily soluble. Furthermore, CAH_{10} is a very difficult phase to nucleate (Capmas et al., 1990; Parr et al., 2005). In addition, the solubility of the CAH_{10} phase is quite high at 20 °C where the analysis was performed (Matschei et al., 2007). Moreover, phases such as CAH_{10} and C_2AH_8 are very difficult to detect by XRD because they have weak crystalline structures in the early stages of hydration (Ukrainczyk et al., 2007). AH_3 could only transform into crystal structures such as gibbsite at the end of high temperatures and in microcrystalline and amorphous structures. For these reasons, it is thought that it is not possible to see these structures during the XRD analysis of the samples.

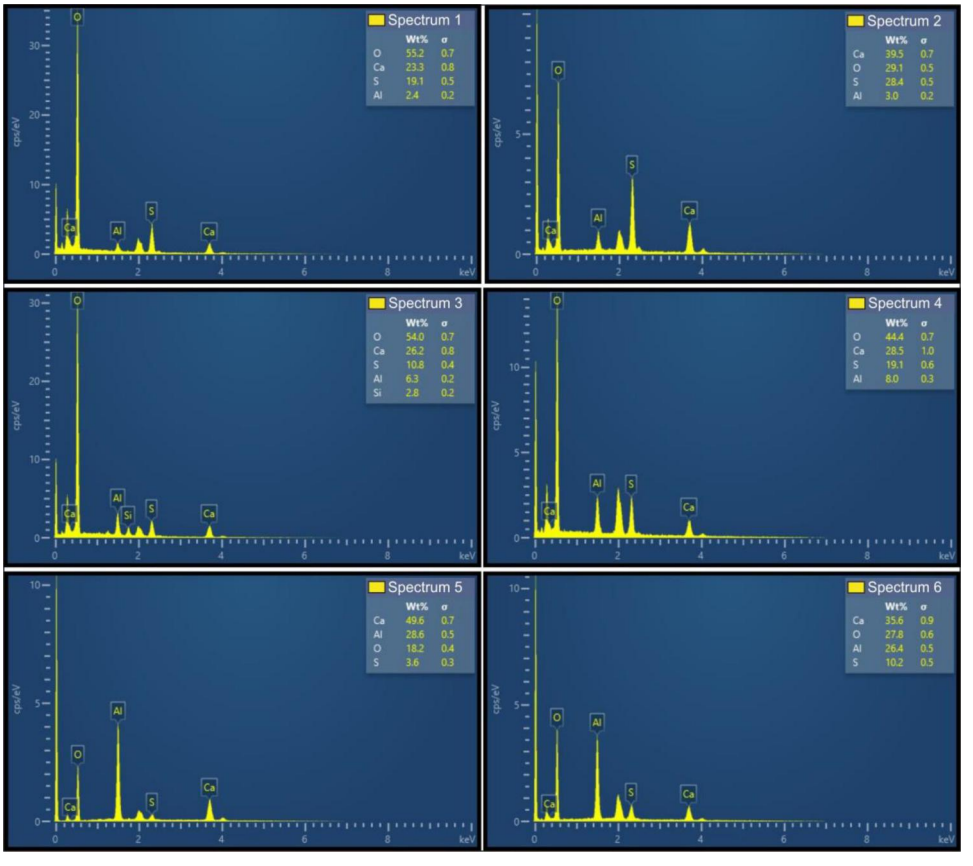

Figure 25. Elementary analyzes of the points shown in Figure 27 (7 kV, in-lens).

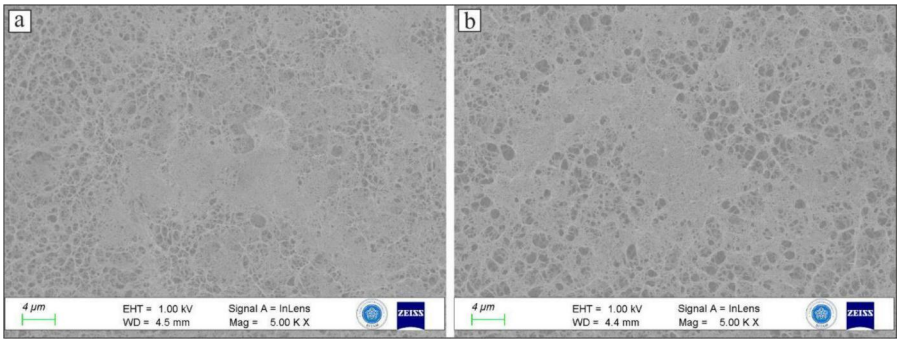

Figure 26. The internal structure of the F60Hh40 sample becomes hollow. (a) 28th day, (b) 90th day.

Figures 18–20 shows the change in the crystal structures of the mixtures prepared with CACs with high $C_{12}A_7$, high CA and high CA_2 ratios, respectively, in advanced ages of hydration. When the figures are examined, it is seen that although the amount of ettringite in the samples decreased a little after the 24th hour until the 28th day, it also increased at the 90th day. Moreover, it is quite clear that substituting 10% SF to binary systems containing 40% Hh increases the amount of ettringite formed, especially at early ages. More clearly, this difference could be seen in 10% SF added ternary systems produced with $C_{12}A_7$ high CAC. In samples produced with CA_2 high CAC, hydration progressed more slowly at 24 h compared to the other two CAC types. However, 40% Hh added binary systems of samples produced with CA_2 high CAC, unlike those produced with $C_{12}A_7$ or CA high CAC, produced more ettringite after 24 h than 10% SF substituted ternary systems (Figure 20).

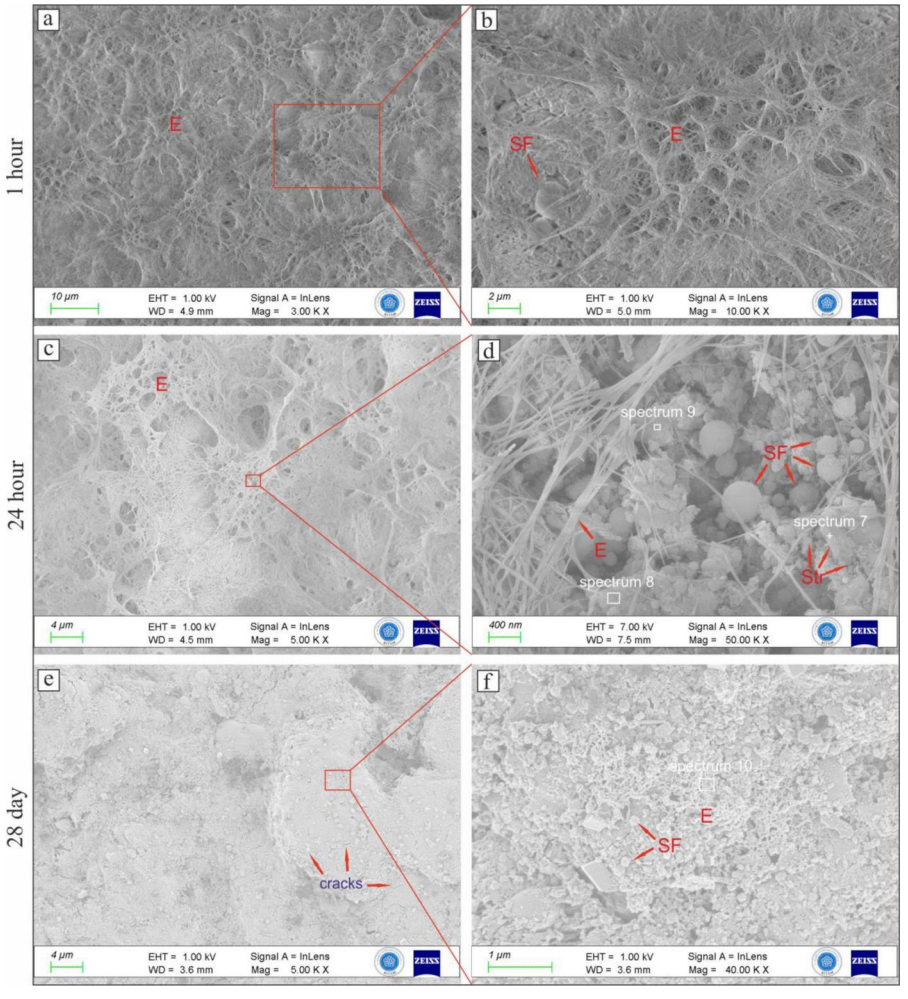

Figure 27. Internal structure images of F60f30Hh10 at different hydration ages. (a, b) 1 h, (c, d) 24 h, (e, f) 28 day (E, ettringite; SF, silica fume; str, strätlingite) (the scales of the images are different).

SF substitution was increased the reaction rates in the other two CAC type while decreasing the reaction rates in samples produced with CA_2 high CAC, especially at early ages, as seen from the isothermal calorimetry results. Furthermore, it is seen that SF also increases the early age strength of samples produced with CA_2 high CAC compared to binary systems, and this clearly reveals that SF has a filling effect that increases the compressive strength in mixtures rather than forming a hydration product at an early age. While the addition of a low rate of SF (10%) accelerates the hydration reaction in $C_{12}A_7$ or CA high CAC types, the addition of a low rate of SF slows the hydration reaction down in mixtures produced with CA_2 high CAC, indicating that the amount of Hh in cement containing high alumina is very important in terms of reaction kinetics.

Another critical issue in the analyzes performed on both *in situ* and late age samples is the change in the amorphous/(amorphous + crystalline) ratio in all hydrated structures according to the sample ages. This ratio, which decreases with the transition of ionisation to phase formation and the rapid formation of crystalline structures such as ettringite in the first hour of hydration, increases with the increase of amorphous structures in the systems at later ages of hydration. On the other hand, as can be seen from the plots, the increase and decrease in the amorphous ratio of some samples with time was also an indication that crystal structure formations and/or crystal structure-amorphous structure transformations (such as ettringite-AFm transformations) within the samples continued with increasing hydration ages. As a result of these transformations, it clearly reveals that changes on the compressive

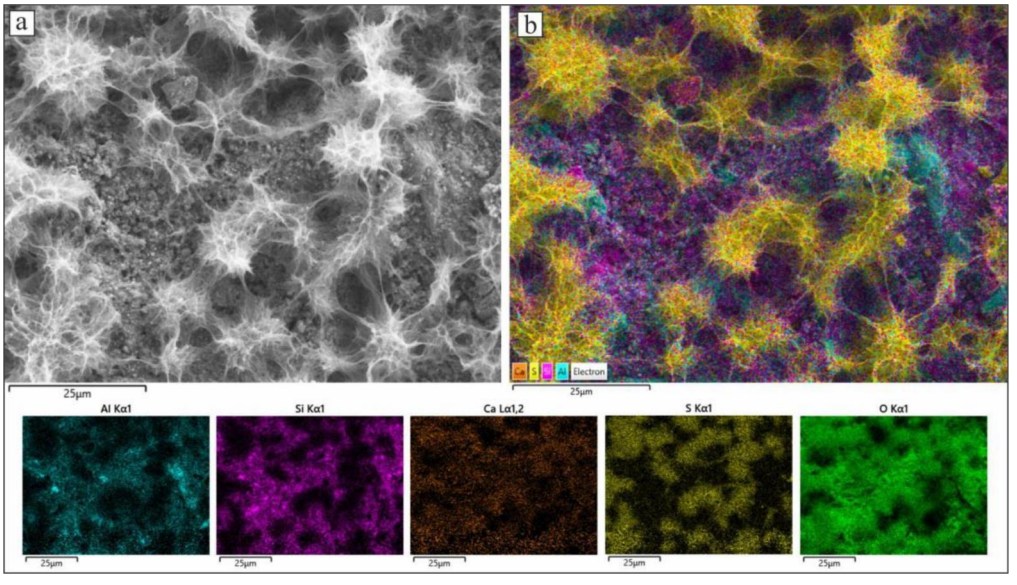

Figure 28. Elementary mapping of the F60f30Hh10 sample at the 1st hour hydration (SE, 7 kV).

strength and the length were occurred in the mortar specimens. The amorphous hydration products formed in the specimens were also examined with TGA and accordingly DTG curves were shown in Figures 21–23.

When the TGA analyzes of the samples were examined, besides ettringite, dihydrate and monocarboaluminate (Mc) (hydrocalumite, thaumasite, etc.) phases and AH_3 were also detected. The peak indicating the presence of Strätlingite (C_2ASH_8) was not seen in binary systems without SF, but was observed in all other systems containing SF. In addition, it could be easily understood from the comparison of the samples containing 30% SF and 10% SF that the increase in the amount of SF in the produced systems leads to the formation of strätlingite at a higher rate. Similarly, the C-A-H structure (CAH_{10}, C_2AH_8, C_3AH_6) was not detected in the TGA results of the samples, like XRD. This situation manifests those metastable and stable phases, which are the main hydration products of CACs, do not form in such ternary and binary systems, even if they are amorphous or weakly crystalline in both early and later ages. In addition, from the TGA analyzes of all prepared samplesshow that the amount of AH_3 in the samples increases with the age of the samples. This increase in AH_3 indicates that the alumina hydrate formed is not in the form of gibbsite, but in a microcrystalline or amorphous structure. Thus, it was evaluated that this increase in the amorphous rates, which was also seen in the XRD analysis of the ternary systems, was largely due to the formation of AH_3.

3.2.3. Internal structure morphology

In this study, FE-SEM and EDS analyzes were performed on the samples prepared by choosing different material ratios, and the internal structure morphologies of the samples were tried to be determined.

3.2.3.1. Internal structure morphology of binary systems. When the internal structures of the binary systems were examined, a similar internal structure was observed in three different cement types. The reticulated crystal structure is prominent in all images (Figure 24). As could be seen from Figure 25, this structure is basically ettringite, considering the presence of Al and S. However, whereas ettringite generally consists of larger diameter needle-shape smooth particles (Poupelloz et al., 2020; Shimada & Young, 2004), the ettringite seen in this study consists of longer fibrils and interlocking reticulated structures. The morphology of hydration products in cementitious materials depends on many factors such as *w*/*b* ratio, temperature, additives and drying methods, as it is known (Zhang et al., 2018). Mainly, it is known that drying methods could change the morphology of crystals that bind large amounts of water like ettringite (Pratt & Ghosh, 1983). Zhang et al. (2018) detected ettringite structures similar to the

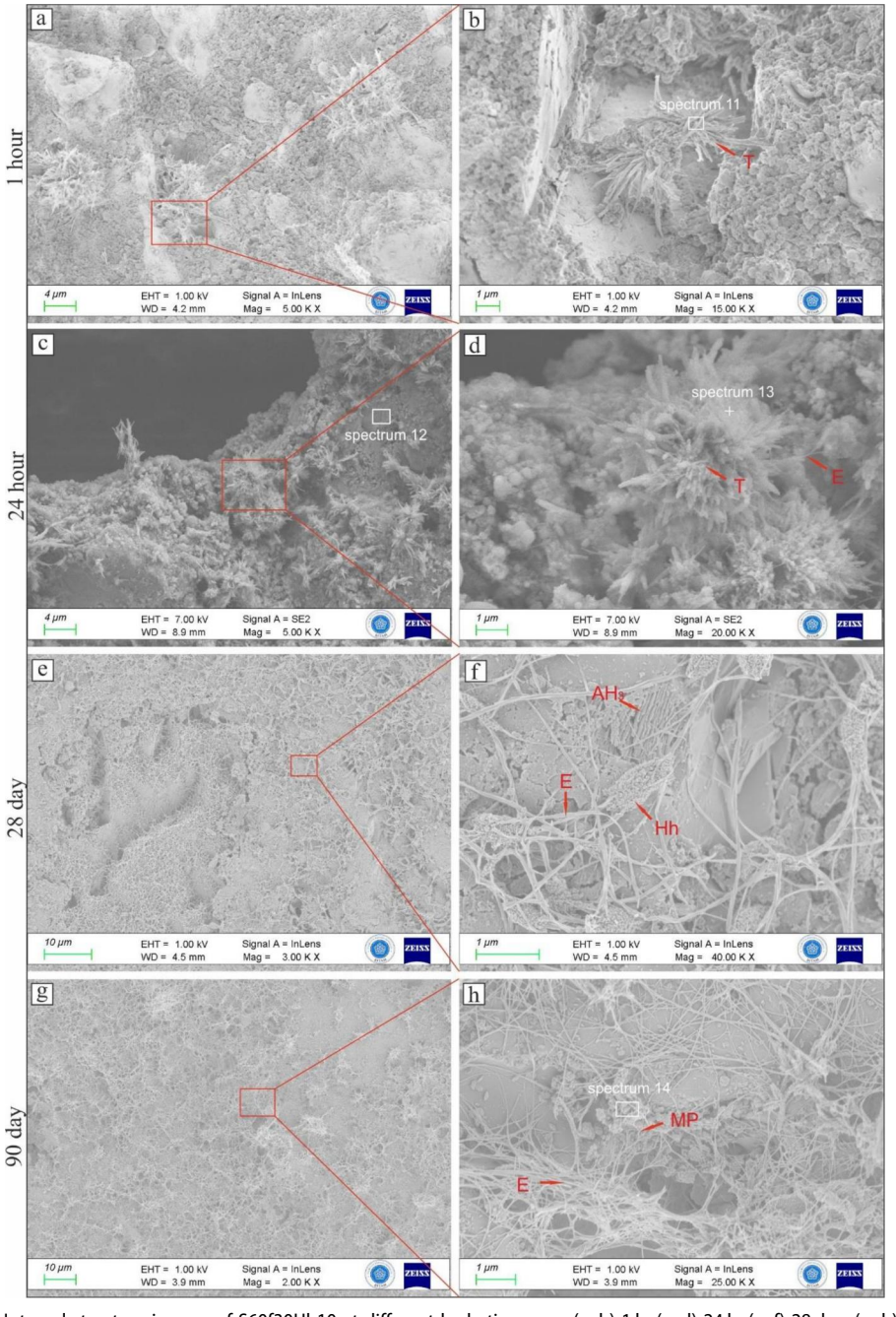

Figure 29. Internal structure images of S60f30Hh10 at different hydration ages. (a, b) 1 h, (c, d) 24 h, (e, f) 28 day, (g, h) 90 day (E, ettringite; T, thaumasite; AH_3, gibbsite; Hh, hemihydrates; MP, minor phases) (the scales of the images are different).

morphology in this study in samples that were suddenly dried with nitrogen, and stated that this sudden drying method caused this reticulated morphology. However, in our study, although isopropanol, which is known to cause less damage to the internal structure, was used instead of a lyophiliser, the long and reticulated ettringite structure shows that the morphology of ettringite is dependent on factors other than the drying method. One of these factors is thought to be stopping hydration at a very early age (Lange et al., 1991).

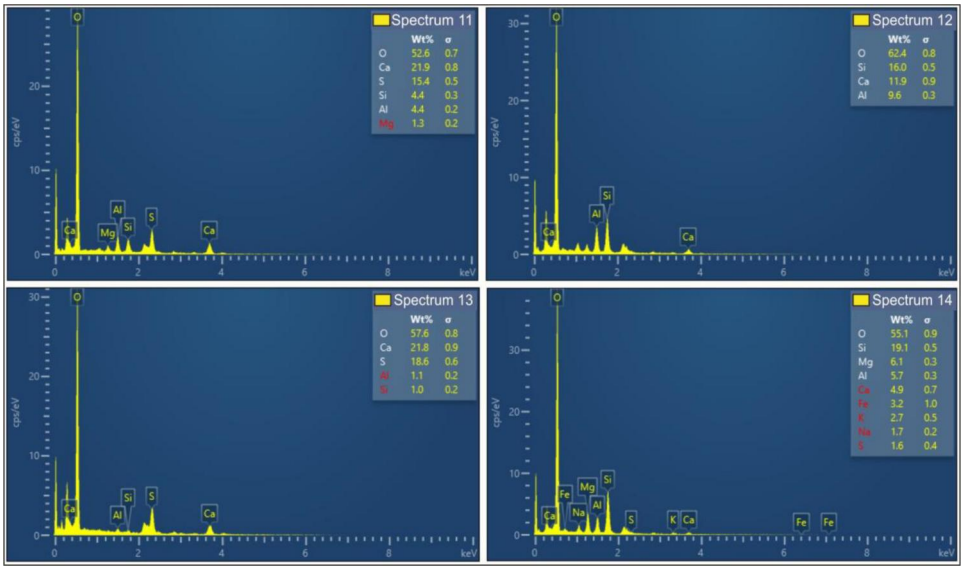

Figure 30. Elementary analysis of the points and area given in Figure 29.

Although it is observed that the inner structure is mainly composed of ettringite at the 24th hour, there are also structures such as AH_3, thaumasite formed on the cement particles. On the 28th day, the ettringite needles are seen in addition to $CaSO_4$. The ettringite structure covered the profile almost homogeneously on day 90. One of the critical issues here is the thinning and elongation of the reticulated ettringite with the age of the sample. As shown in Figure 26, as a result of this elongation and thinning, the microstructure contains more numerous and, more importantly, larger dimensional voids at the advanced ages of the samples. This is thought to be one of the reasons for the fluctuations in compressive strength of many of the samples, particularly those containing high levels of Hh.

3.2.3.2. Internal structure morphology of ternary systems. Incontrast to binary systems, the most striking difference in the internal structure images of ternary systems containing SF was that they had a much denser internal structure (Figure 27). The voids of the reticulated structure of ettringite in binary systems were not observed in ternary systems containing high amount of SF. Internal structure images in ternary systems proved the filling effect of SF, which is also seen in the hydration kinetics and compressive strengths of the samples.

In Figure 28, the internal structures of the samples produced with a $C_{12}A_7$ high CAC, SF, Hh, respectively, 60%, 30%, 10% by weight were given according to their hydration ages. It is observed that a reticulated ettringite structure was formed in the internal structure of the samples from the first hour. However, unlike the binary system, the ettringite structure could not cover the entire surface. This situation was clearly revealed the importance of gypsum in ettringite dominant systems. The ettringite structures formed in the system, whose hydration was stopped at the end of the first hour, can be easily seen with elemental mapping on the sample F60f30Hh10. The S/Al ratio in these structures, which are seen in yellow colours (Figure 28), was quite high.

The internal structure images of the S60f30Hh10 were given in Figure 29. Ettringite formations were observed from the first hour in samples produced with CA high CAC, similar to the samples produced with $C_{12}A_7$ high CAC. On the other hand, the difference in the proportions of cement oxides also affected the structures of the formed ettringites. In these samples, ettringite began to form in the end regions of structures which, according to EDX analysis, resembled thaumasite. The thaumasite structure when the sample was still in the first hour of hydration seen in Figure 29b, grew together with the ettringite needles as seen in Figure 29d. Moreover, it is seen that the ettringite structure was wrapped in long needles in the form of a reticulated structure on the dough at the 28th and 90th days. In addition, ettringite is also nucleated on Hh particles (Figure 29f and h). From the spectral elemental analysis of the points

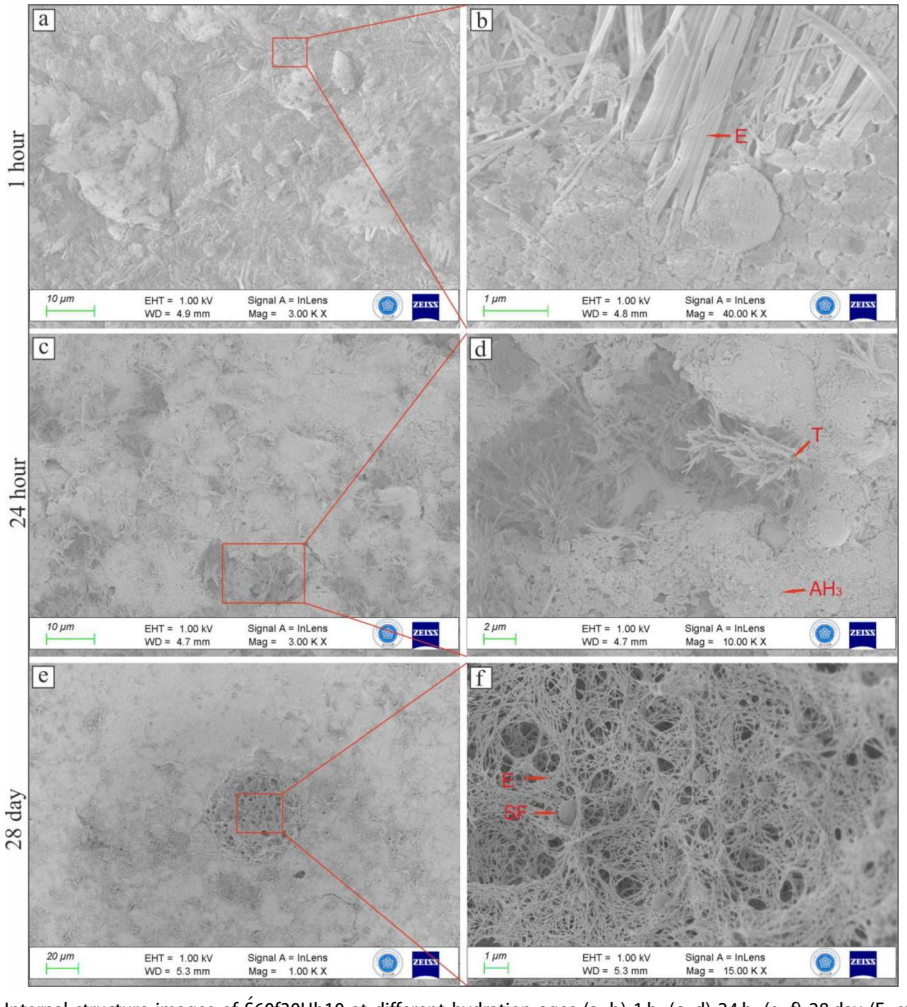

Figure 31. Internal structure images of Ś60f30Hh10 at different hydration ages (a, b) 1 h, (c, d) 24 h, (e, f) 28 day (E, ettringite; T, thaumasite; AH_3, gibbsite; SF, silica fume) (the scales of the images are different).

marked in Figure 29, the silica content of the floral structures consisting mainly of thaumasite was also higher containing high amount of SF (Figure 30).

The internal structure images of the Ś60f30Hh10 produced with CA_2 high CAC at different hydration ages were given in Figure 31. Correspondingly to the XRD results, Ettringite formation was less at the first hour of hydration when compared to other samples. The cement and SF particles in the sample can be easily seen in the first hour of hydration (Figure 31a). However, ettringite needles formed in the first hour of hydration were larger diameter and smooth particles in contrast to the reticulated ettringite structure formed from mixtures produced with the other two CAC (Figure 31b). In addition, the S/Al ratio of this ettringite structure is close to 1 unlike the others. However, it is seen that the ettringite structures formed in the sample develop mostly within the voids as shown in Figure 31c–f.

4. Conclusions

Within the scope of this study, binary systems were created by using CACs with different oxide types and ratios and Hh gypsum, and triple systems were created by adding SF to these systems. In addition, by using these materials in different ratios, the effects of these different ratios on the hydration kinetics and products of the systems and the morphology of the internal structure were investigated. On the other hand, in order to detect the hydration products of the systems from the early ages, the setting

accelerator (Li_2SO_4) is used to accelerate the early age strength. As a result of the analysis carried out on the samples, the following findings were obtained;

- In binary and ternary systems, the main hydration product is ettringite, both in early and later ages. Except for ettringite, the samples did not encounter metastable and/or stable calcium alumina hydrated structures that cause strength and porosity changes.
- The presence of peaks indicating ettringite formation could be seen from the in-situ XRD results, considering the first minutes of hydration. However, both TGA and FE-SEM analyzes of samples whose hydration was stopped after 1 h of hydration indicate that the formation of thaumasite, and hydrocalumite, is also relatively high. It is thought that these two different results may have resulted from different reasons; Firstly, because the XRD reference peaks of thaumasite and hydrocalumite are very close to each other, it is very difficult to distinguish between the nested peaks in XRD analyzes on both in-situ and hardened samples. Secondly, the reason for the lower amount of ettringite in the TGA analysis performed on the samples whose hydration was stopped and dried may be due to the AFt – AFm phase transformations due to this drying. Thus, it can be said that all AFt structures were formed at a higher rate in the first stages of hydration from XRD and FE-SEM analyzes. However, it is quite difficult to completely separate the amounts of these structures in the total phase from each other quantitatively.
- In systems where Hh is used at high ratios, a high early strength was observed as a result of the rapid development of ettringite. In addition, as the ettringite continued to form, the expansions in the systems continued to increase. On the other hand, the shrinkage may have occurred due to the sulphate depletion caused by rapid formation of ettringite in the first minutes and the AFt-AFm transformations later in the specimens contain high CAC/Hh ratio. This conversion was also seen to some extent in the calorimeter results.
- The fact that the compressive strengths of CA high CAC are higher than those of $C_{12}A_7$ high CAC, which react very rapidly, suggests that the increase in the Al/Ca ratio in the hydration products has a positive effect on the compressive strength. The late strength of CA_2 high CAC with slow dissolution rate is higher than the other two CACs confirms this result. It is also observed that the formation of AH_3 significantly increases the compressive strength of the specimens. The SF used in the mixtures has considerably increased the early age strength of the systems, as it has both a filling effect and creates an extra area for the nucleation of hydration products. This nucleation effect of SF is understood from the fact that the cumulative heat energies of the ternary systems determined by isothermal calorimetry are higher than the binary systems. The filling effect in the mixtures can be easily seen from the density of the internal structure images of the systems containing SF. On the other hand, the amount of expansion in the Ś60f10Hh30 is higher than in the F60f10Hh30 at late ages is another proof that SD accelerates the reaction of CA_2, which can react very slowly, and can form higher AH_3 and ettringite due to the high alumina content.
- Another consequence of the formation of strätlingite in mixtures using a high ratio of SF was that the specimens prepared in this way are more stable in terms of dimensional stability. Since strätlingite is a much more stable structure unlike ettringite, the relative length changes in specimens containing high ratios of SF were also less than SF not using ones.

When comparing the results obtained from the three cements, it may be appropriate to use CA high CAC when very high early strength is expected, and CA_2 high CAC when high ultimate strength and high stability are expected from ternary systems. $C_{12}A_7$ high CAC can be used in the production of some non-structural repair mortars where high early strength is desired but very high stability is not expected, as it is a cheaper cement type compared to other cement types.

In the light of the results obtained from this study, the following suggestions will contribute to this field;

- The effect of AH_3 on mechanical behaviours and its long-term stability should be analyzed. It should also be investigated whether there is any relationship with the formation of strätlingite.
- The interaction effects on the hydration properties and products of highly reactive oxides of CACs should be further investigated.

- The effects of changes in the Al/Ca ratio on the morphology of the hydration products should be studied in detail.

Acknowledgements

This study was prepared from the PhD thesis of Murat Saydan with the advisor of Ülkü Sultan Keskin and co-advisor of Burak Uzal, which was accepted by Konya Technical University, Graduate Education Institute, Department of Civil Engineering.

Disclosure statement

The authors declare that they have no known competing financial interests or personal relationships that could have appeared to influence the work reported in this paper.

Funding

This study was funded by the Scientific and Technological Research Council of Turkey (TUBITAK) [ARDEB 1002 grant number 119M159]; and the researcher training program by Council of Higher Education (Turkey) [grant number 2016-ÖYP-049].

ORCID

Murat Saydan http://orcid.org/0000-0003-3598-468X

Data availability statement

The data that support the findings of this study are available from the corresponding author, [MS], upon reasonable request.

References

Amathieu, L., Bier, T. A., & Scrivener, K. L. (2001). Mechanisms of set acceleration of Portland cement through CAC addition. *Calcium Aluminate Cements 2001*: Proceedings of the International Conference on Calcium Aluminate Cements (CAC), Heriot-Watt University, 16–19 July 2001 (pp. 303–317).

Anderson, M. J. (2017). Permutational Multivariate Analysis of Variance (PERMANOVA). In *Wiley StatsRef: Statistics reference online* (pp. 1–15). https://doi.org/10.1002/9781118445112.stat07841

Anderson, K., & Akono, A. T. (2017). Microstructure–toughness relationships in calcium aluminate cement–polymer composites using instrumented scratch testing. *Journal of Materials Science*, *52*(22), 13120–13132. https://doi.org/10.1007/S10853-017-1416-8/FIGURES/10

ASTM C109/C109M-20b. (2020). *Standard test method for compressive strength of hydraulic cement mortars (Using 2-in. or [50 mm] cube specimens)*. ASTM International. http://www.astm.org/cgi-bin/resolver.cgi?C109C109M

ASTM C490/490M-21. (2021). *Standard practice for use of apparatus for the determination of length change of hardened cement paste, mortar, and concrete*. ASTM International.

Baquerizo, L. G., Matschei, T., & Scrivener, K. L. (2016). Impact of water activity on the stability of ettringite. *Cement and Concrete Research*, *79*, 31–44. https://doi.org/10.1016/j.cemconres.2015.07.008

Bizzozero, J. (2014). *Hydration and dimensional stability of calcium aluminate cement based systems* [Doctoral thesis]. École Polytechnique Fédérale de Lausanne.

Brooks, S., & Sharp, J. H. (1990). Ettringite-based cements. In R. J. Mangabhai (Ed.). *Proceedings of the International Symposium Held at Queen Mary and Westfield College, University of London, 9–11 July 1990, and Dedicated to the Late Dr H. G. Midgley*. E.& F.N. SPON.

Brown, P. W., & Bothe, J., Jr.,(1993). The stability of ettringite. *Advances in Cement Research*, *5*(18), 47–63. https://doi.org/10.1680/adcr.1993.5.18.47

Capmas, A., Menetrier-Sorrentino, D., & Damidot, D. (1990). Effect of temperature on setting time of calcium aluminate cements. *Calcium Aluminate Cements*, 65–80.

Cecilie, E., & Hansen, S. (2001). Expansive properties of ettringite in a mixture of calcium aluminate cement, Portland cement and b-calcium sulfate hemihydrate. *Cement Concrete Res*, *31*, 157–261.

Christensen, A. N., Jensen, T. R., & Hanson, J. C. (2004). Formation of ettringite, $Ca_6Al_2SO_4$ $3OH_{12}{\cdot}26H_2O$, AFt, and monosulfate, $Ca_4Al_2O_6SO_4{\cdot}14H_2O$, AFm-14, in hydrothermal hydration of Portland cement and of calcium aluminum oxide – Calcium sulfate dihydrate mixtures studied by in situ synchrotron X-ray powder diffraction. *Journal of Solid State Chemistry*, *177*(6), 1944–1951. https://doi.org/10.1016/j.jssc.2003.12.030

Chung, F. H. (1973). A new X-ray diffraction method for quantitative multicomponent analysis. *Advances in X-Ray Analysis*, *17*, 106–115. https://doi.org/10.1154/S0376030800005231

Damidot, D., Lothenbach, B., Herfort, D., & Glasser, F. P. (2011). Thermodynamics and cement science. *Cement and Concrete Research*, *41*(7), 679–695. https://doi.org/10.1016/j.cemconres.2011.03.018

Deng, G., He, Y., Lu, L., & Hu, S. (2020). Evolution of aluminate hydrate phases in fly ash-cement system under the sulfate conditions. *Construction and Building Materials*, *252*, 119045. https://doi.org/10.1016/j.conbuildmat.2020.119045

Ding, J., Fu, Y., & Beaudoin, J. J. (1995). Strätlingite formation in high alumina cement - silica fume systems: Significance of sodium ions. *Cement and Concrete Research*, *25*(6), 1311–1319. https://doi.org/10.1016/0008-8846(95)00124-U

Ding, J., Fu, Y., & Beaudoin, J. J. (1996). Study of hydration mechanisms in the high alumina cement – Sodium silicate system. *Cement and Concrete Research*, *26*(5), 799–804. https://doi.org/10.1016/S0008-8846(96)85017-4

Fernández-Carrasco, L., & Vázquez, E. (2009). Reactions of fly ash with calcium aluminate cement and calcium sulphate. *Fuel*, *88*(9), 1533–1538. https://doi.org/10.1016/j.fuel.2009.02.018

Gosselin, C. (2009). *Microstructural development of calcium aluminate cement based systems with and without supplementary cementitious materials* [Doctoral thesis]. École Polytechnique Fédérale de Lausanne,

Gu, P., Beaudoin, J. J., Quinn, E. G., & Myers, R. E. (1997). Early strength development and hydration of ordinary portland cement/calcium aluminate cement pastes. *Advanced Cement Based Materials*, *6*(2), 53–58. https://doi.org/10.1016/S1065-7355(97)00008-4

Gu, P., Fu, Y., & Beaudoin, J. J. (1994). A study of the hydration and setting behaviour of OPC-HAC pastes. *Cement and Concrete Research*, *24*(4), 682–694. https://doi.org/10.1016/0008-8846(94)90192-9

Hall, C., Barnes, P., Billimore, A. D., Jupe, A. C., & Turrillas, X. (1996). Thermal decomposition of ettringite Ca6 $[Al(OH)_6]2(SO_4)3{\cdot}26H_2O$. *Journal of the Chemical Society – Faraday Transactions*, *92*(12), 2125–2129. https://doi.org/10.1039/FT9969202125

Hand, D. J., & Taylor, C. C. (1987). *Multivariate analysis of variance and repeated measures: A practical approach for behavioural scientists*. CRC press.

Heikal, M., Radwan, M. M., & Morsy, M. S. (2004). Influence of curing temperature on the physicomechanical, characteristics of calcium aluminate cement with air-cooled slag or water-cooled slag. *Ceramics - Silikaty*, *48*, 185–196.

Hentschel, G., & Kuzel, H. J. (1976). Straetlingit, 2CAO. AL_2O_3. SiO_2. $8H_2O$. *Neues Jahrbuch für Mineralogie, Monatshefte*, 326–330.

Hidalgo, A., García, J. L., Alonso, M., Fernández, L., & Andrade, C. (2009). Microstructure development in mixes of calcium aluminate cement with silica fume or fly ash. *Journal of Thermal Analysis and Calorimetry*, *96*(2), 335–345. https://doi.org/10.1007/s10973-007-8439-3

Hou, D., & Li, T. (2018). Influence of aluminates on the structure and dynamics of water and ions in the nanometer channel of calcium silicate hydrate (C–S–H) gel. *Physical Chemistry Chemical Physics*, *20*(4), 2373–2387. https://doi.org/10.1039/C7CP06985E

Hou, D., Li, T., & Wang, P. (2018). Molecular dynamics study on the structure and dynamics of NaCl solution transport in the nanometer channel of CASH Gel. *ACS Sustainable Chemistry & Engineering*, *6*(7), 9498–9509. https://doi.org/10.1021/acssuschemeng.8b02126

Hubbard, C. R., & Snyder, R. L. (1988). RIR - Measurement and use in quantitative XRD. *Powder Diffraction*, *3*(2), 74–77. https://doi.org/10.1017/S0885715600013257

Ideker, J. H., Scrivener, K. L., Fryda, H., & Touzo, B. (2019). Calcium aluminate cements. In *Lea's chemistry of cement and concrete* (pp. 537–584). Elsevier. https://doi.org/10.1016/B978-0-08-100773-0.00012-5

Kelley, K. K., Southard, J. C., & Anderson, C. T. (1941). *Thermodynamic properties of gypsum and its dehydration products*. US Government Printing Office

Kim, C. B., Kim, B. K., & Choi, S. C. (2007). Characteristics of calcium trisulphoaluminate hydrates for rapid hardening of cement composites. In *Materials science forum* (pp. 669–672). Trans Tech Publ. https://doi.org/10.4028/www.scientific.net/MSF.544-545.669

Kirca, Ö., Özgür Yaman, I., & Tokyay, M. (2013). Compressive strength development of calcium aluminate cement-GGBFS blends. *Cement and Concrete Composites*, *35*(1), 163–170. https://doi.org/10.1016/j.cemconcomp.2012.08.016

Lange, D. A., Sujata, K., & Jennings, H. M. (1991). Observations of wet cement using electron microscopy. *Ultramicroscopy*, *37*(1–4), 234–238. https://doi.org/10.1016/0304-3991(91)90021-W

Li, H., Xu, C., Li, L., Chen, Q., Yang, X., Wang, W., & Liu, R. (2020). Insight into the influences of β-hemihydrate and dihydrate gypsum on the properties and phase conversion of white calcium aluminate cement. *Construction and Building Materials*, *263*, 120106. https://doi.org/10.1016/j.conbuildmat.2020.120106

Lothenbach, B., Pelletier-Chaignat, L., & Winnefeld, F. (2012). Stability in the system CaO-Al_2O_3-H_2O. *Cement and Concrete Research*, *42*(12), 1621–1634. https://doi.org/10.1016/j.cemconres.2012.09.002

Lu, C., Shen, J., Fu, Q., & Mo, J. (2023). Research on radial crack propagation of railway brake disc under emergency braking conditions. *Engineering Failure Analysis*, *143*, 106877. https://doi.org/10.1016/j.engfailanal.2022.106877

Majumdar, A. J., Edmonds, R. N., & Singh, B. (1990). Hydration of Secar 71 aluminous cement in presence of granulated blast furnace slag. *Cement and Concrete Research*, *20*(1), 7–14. https://doi.org/10.1016/0008-8846(90)90111-A

Mangabhai, R. J. (Ed.) (1990). Calcium aluminate cements. *Proceedings of a Symposium dedicated to HG Midgley, London, July 1990* (1st ed.). Taylor & Francis.

Matschei, T., Lothenbach, B., & Glasser, F. P. (2007). Thermodynamic properties of Portland cement hydrates in the system CaO-Al_2O_3-SiO_2-$CaSO_4$-$CaCO_3$-H_2O. *Cement and Concrete Research*, *37*(10), 1379–1410. https://doi.org/10.1016/j.cemconres.2007.06.002

Mehta, P. K., & Monteiro, P. J. M. (2014). *Concrete: Microstructure, properties, and materials*., McGraw-Hill Education.

Midgley, H. G., & Bhaskara Rao, P. (1978). Formation of stratlingite, $2CaO.SiO_2.Al_2O_3.8H_2O$, in relation to the hydration of high alumina cement. *Cement and Concrete Research*, *8*(2), 169–172. https://doi.org/10.1016/0008-8846(78)90005-4

Mi̯rki̯n, L. I. (1961). *Handbook of X-ray structural analysis of polycrystals*. Springer.

Okoronkwo, M. U., & Glasser, F. P. (2016a). Stability of strätlingite in the CASH system. *Materials and Structures*, *49*(10), 4305–4318. https://doi.org/10.1617/s11527-015-0789-x

Okoronkwo, M. U., & Glasser, F. P. (2016b). Strätlingite: Compatibility with sulfate and carbonate cement phases. *Materials and Structures*, *49*(9), 3569–3577. https://doi.org/10.1617/s11527-015-0740-1

Osborne, G. J, (1994). BRECEM: A rapid hardening cement based on high alumina cement. *Proceedings of the Institution of Civil Engineers - Structures and Buildings*, *104*(1), 93–100. https://doi.org/10.1680/istbu.1994.25683

Osborne, G. J., & Singh, B. (1995). The Durability of Concretes Made with BRECEM Cement Comprised of Blends of CAC and GGBFS. Proceedings of the 5th CANMET/ACI International Conference on Fly Ash, Silica Fume, Slag and Natural Pozzolans in Concrete (pp. 885–909).

Parr, C., Simonin, F., Touzo, B., Wohrmeyer, C., Valdelièvre, B., & Namba, A. (2005). The impact of calcium aluminate cement hydration upon the properties of refractory castables. *Journal of Technical Association of Refractories Japan*, *25*, 78–88.

Passaglia, E., & Turconi, B. (1982). Silicati ed altriminerali di Montalto di Castro (Viterbo). *Rivista Mineralogica Italiana*, *4*, 97–110.

Poupelloz, E., Gauffinet, S., & Nonat, A. (2020). Study of nucleation and growth processes of ettringite in diluted conditions. *Cement and Concrete Research*, *127*, 105915. https://doi.org/10.1016/j.cemconres.2019.105915

Pratt, P. L., & Ghosh, A. (1983). Electron microscope studies of Portland cement microstructures during setting and hardening. *Philosophical Transactions of the Royal Society of London. Series A, Mathematical and Physical Sciences*, *310*, 93–103.

Qoku, E., Bier, T. A., & Westphal, T. (2017). Phase assemblage in ettringite-forming cement pastes: A X-ray diffraction and thermal analysis characterization. *Journal of Building Engineering*, *12*, 37–50. https://doi.org/10.1016/j.jobe.2017.05.005

Quillin, K., Osborne, G., Majumdar, A., & Singh, B. (2001). Effects of w/c ratio and curing conditions on strength development in BRECEM concretes. *Cement and Concrete Research*, *31*(4), 627–632. https://doi.org/10.1016/S0008-8846(00)00494-4

Rayment, D. L., & Majumdar, A. J. (1994). Microanalysis of high-alumina cement clinker and hydrated HAC/SLAG mixtures. *Cement and Concrete Research*, *24*(2), 335–342. https://doi.org/10.1016/0008-8846(94)90060-4

Renaudin, G., Filinchuk, Y., Neubauer, J., & Goetz-Neunhoeffer, F. (2010). A comparative structural study of wet and dried ettringite. *Cement and Concrete Research*, *40*(3), 370–375. https://doi.org/10.1016/j.cemconres.2009.11.002

Rodger, S. A., & Double, D. D. (1984). The chemistry of hydration of high alumina cement in the presence of accelerating and retarding admixtures. *Cement and Concrete Research*, *14*(1), 73–82. https://doi.org/10.1016/0008-8846(84)90082-6

Rolnick, L. S. (1954). *The stability of gypsum and anhydrate* [Unpublished doctoral Thesis]. Massachusetts Institute of Technology.

Scrivener, K. (2003). Calcium aluminate cements. In *Advanced concrete technology* (pp. 1–31). Elsevier Ltd. https://doi.org/10.1016/B978-075065686-3/50278-0

Scrivener, K. L., & Capmas, A. (2003). Calcium aluminate cements. In *Lea's chemistry of cement and concrete* (pp. 713–782). Elsevier Ltd. https://doi.org/10.1016/B978-075066256-7/50025-4

Shimada, Y., & Young, J. F. (2004). Thermal stability of ettringite in alkaline solutions at 80 °C. *Cement and Concrete Research*, *34*(12), 2261–2268. https://doi.org/10.1016/j.cemconres.2004.04.008

Singh, B., Majumdar, A. J., & Quillin, K. (1999). Properties of BRECEM ten-year results. *Cement and Concrete Research*, *29*(3), 429–433. https://doi.org/10.1016/S0008-8846(98)00227-0

Singh, V. K., & Glasser, F. P. (1988). High-temperature reversible moisture uptake in calcium aluminate, $Ca_{12}Al_{14}O_{33}$-x(OH)2x. *Ceramics International*, *14*(1), 59–62. https://doi.org/10.1016/0272-8842(88)90019-3

Snelus, G. J., Gibb, T., Swann, J. C., Smith, H., & Whamond, W. (1888). British Patent 10312.

Son, H. M., Park, S. M., Jang, J. G., & Lee, H. K. (2018). Effect of nano-silica on hydration and conversion of calcium aluminate cement. *Construction and Building Materials*, *169*, 819–825. https://doi.org/10.1016/j.conbuildmat.2018.03.011

Son, H. M., Park, S., Kim, H. Y., Seo, J. H., & Lee, H. K. (2019). Effect of $CaSO_4$ on hydration and phase conversion of calcium aluminate cement. *Construction and Building Materials*, *224*, 40–47. https://doi.org/10.1016/j.conbuildmat.2019.07.004

Sun, W., Zhou, F., Liu, J., & Shao, J. (2022). Experimental study on Portland cement/calcium sulfoaluminate binder of paste filling. *European Journal of Environmental and Civil Engineering*, *26*(5), 1706–1721. https://doi.org/10.1080/19648189.2020.1731712

Tang, Z.-Z., Chen, G., & Alekseyenko, A. V. (2016). PERMANOVA-S: Association test for microbial community composition that accommodates confounders and multiple distances. *Bioinformatics (Oxford, England)*, *32*(17), 2618–2625. https://doi.org/10.1093/bioinformatics/btw311

Torréns-Martín, D., & Fernández-Carrasco, L. (2013). Effect of sulfate content on cement mixtures. *Construction and Building Materials*, *48*, 144–150. https://doi.org/10.1016/j.conbuildmat.2013.05.106

Torréns-Martín, D., Fernández-Carrasco, L., & Blanco-Varela, M. T. (2013). Conduction calorimetric studies of ternary binders based on Portland cement, calcium aluminate cement and calcium sulphate. *Journal of Thermal Analysis and Calorimetry*, *114*(2), 799–807. https://doi.org/10.1007/s10973-013-3003-9

Tzouvalas, G., Dermatas, N., & Tsimas, S. (2004). Alternative calcium sulfate-bearing materials as cement retarders: Part I. Anhydrite. *Cement and Concrete Research*, *34*(11), 2113–2118. https://doi.org/10.1016/j.cemconres.2004.03.020

Ukrainczyk, N., Matusinovic, T., Kurajica, S., Zimmermann, B., & Sipusic, J. (2007). Dehydration of a layered double hydroxide—C_2AH_8. *Thermochimica Acta*, *464*(1–2), 7–15. https://doi.org/10.1016/j.tca.2007.07.022

Xu, L., Wang, P., & Zhang, G. (2012a). Calorimetric study on the influence of calcium sulfate on the hydration of Portland cement–calcium aluminate cement mixtures. *Journal of Thermal Analysis and Calorimetry*, *110*(2), 725–731. https://doi.org/10.1007/s10973-011-1920-z

Xu, L., Wang, P., & Zhang, G. (2012b). Formation of ettringite in Portland cement/calcium aluminate cement/calcium sulfate ternary system hydrates at lower temperatures. *Construction and Building Materials*, *31*, 347–352. https://doi.org/10.1016/j.conbuildmat.2011.12.078

Ye, F., He, B., Tian, C., Wang, J., Han, X., Song, G., & Wang, Q. (2022). Analysis of mechanism, properties and existing problems of liquid setting accelerators. *European Journal of Environmental and Civil Engineering*, *26*(16), 8366–8389. https://doi.org/10.1080/19648189.2022.2026822

Zhang, Z., Scherer, G. W., & Bauer, A. (2018). Morphology of cementitious material during early hydration. *Cement and Concrete Research*, *107*, 85–100. https://doi.org/10.1016/j.cemconres.2018.02.004

Zhang, S., Xu, X., Memon, S. A., Dong, Z., Li, D., & Cui, H. (2018). Effect of calcium sulfate type and dosage on properties of calcium aluminate cement-based self-leveling mortar. *Construction and Building Materials*, *167*, 253–262. https://doi.org/10.1016/j.conbuildmat.2018.01.146

Zhang, X., Yang, Y., & Ong, C. K. (1997). Study of early hydration of OPC-HAC blends by microwave and calorimetry technique. *Cement and Concrete Research*, *27*(9), 1419–1428. https://doi.org/10.1016/S0008-8846(97)00124-5

Zhou, Q., & Glasser, F. P. (2001). Thermal stability and decomposition mechanisms of ettringite at $<120\,^{\circ}C$. *Cement and Concrete Research*, *31*(9), 1333–1339. https://doi.org/10.1016/S0008-8846(01)00558-0

Zhou, Q., Lachowski, E. E., & Glasser, F. P. (2004). Metaettringite, a decomposition product of ettringite. *Cement and Concrete Research*, *34*(4), 703–710. https://doi.org/10.1016/j.cemconres.2003.10.027

Zhu, Z., Wang, Z., Xu, L., Peng, X., Zhou, Y., & Wu, K. (2022). Phase-dependent study of chloride binding capacity and its relation to the properties of CAC. *Journal of Building Engineering*, *46*, 103718. https://doi.org/10.1016/j.jobe.2021.103718